

University Medical Center Ulm
Department of Internal Medicine II
Prof. Dr. med. Wolfgang Rottbauer
Molecular Cardiology
Prof. Dr. rer. nat. Steffen Just

**Targeted loss of
SET domain-containing protein 5
impairs cardiac morphology and
function *in vivo***

Dissertation submitted in partial fulfilment of the requirements for the
degree of “doctor medicinae” (Dr. med.) of the
Medical Faculty of Ulm University

Sabine Schreiber
Born in Esslingen am Neckar

Ulm
2018

Current Dean:

Prof. Dr. rer. nat. Thomas Wirth

First Reviewer:

Prof. Dr. rer. nat. Steffen Just

Second Reviewer:

Prof. Dr. med. Jochen Weishaupt

Day doctorate awarded:

11th January 2019

to life

Table of Contents

Abbreviations.....	VI
1 Introduction	1
1.1 Cardiovascular disease (CVD).....	1
1.2 Epigenetic regulation of gene expression in cardiovascular disease.....	1
1.3 The family of SET domain-containing proteins	2
1.4 SET domain-containing protein 5.....	3
1.5 The zebrafish <i>danio rerio</i> – an ideal model organism to detect cardiac phenotypes	4
1.6 Forward and reverse genetics in zebrafish	5
1.7 Aim of work	6
2 Material and Methods.....	7
2.1 Material	7
2.2 Methods	22
3 Results	33
3.1 <i>SETD5</i> is conserved among species	33
3.2 <i>Setd5</i> is ubiquitously expressed in zebrafish from early developmental stages on	35
3.3 Localization of <i>Setd5</i> on cellular level	37
3.4 Knockdown of <i>setd5</i> leads to heart defects during early zebrafish development.....	39
3.5 Knockdown of <i>setd5</i> leads to cardiac arrhythmia	41
3.6 Loss of <i>setd5</i> results in heart morphology changes.....	43
3.7 <i>Setd5</i> is not responsible for endocardial development	45
3.8 Knockdown of <i>setd5</i> shows normal cardiomyocyte differentiation and specification.....	46
3.9 <i>Setd5</i> is essential to maintain cardiac contractile function in zebrafish ..	49
3.10 <i>Setd5</i> is involved in histone methylation and acetylation.....	53

4	Discussion	55
4.1	<i>Setd5</i> shows cross-species homology	55
4.2	Loss of <i>Setd5</i> leads to defects in cardiac morphology and function	56
4.3	<i>Setd5</i> influences the chromatin state	58
4.4	<i>Setd5</i> presumably functions in Notch Signaling.....	59
5	Summary	62
6	References	63
	Acknowledgements	72
	Statutory declaration	72
	Curriculum vitae	74

Abbreviations

°C	degree Celsius
%	percentage
A	atrium
amhc	atrial myosin heavy chain
au	arbitrary unit
AVC	atrioventricular canal
bp	base pair
bpm	beats per minute
BSA	bovine albumin serum
cDNA	complementary DNA
cmhc2	cardiac myosin light chain 2
CRISPR	clustered, regularly interspaced, short palindromic repeat
CVD	Cardiovascular disease
DAPI	4',6-diamidino-2-phenylindole
DEPC	Diethyl pyrocarbonate
DMSO	Dimethylsulfoxid
DNA	Deoxyribonucleic acid
E	embryonic age of mice
E3	embryo media
E.coli	Escherichia coli
EDTA	Ethydiamine-tetra-acetate
eGFP	enhanced Green Fluorescent Protein
ENU	Ethyl-Nitrosourea
FCS	fetal calf serum
FS	fractional shortening
g	gram
HAT	Histone acetyltransferase
HDAC	Histone deacetyltransferase
HMT	Histone methyltransferase
hpf	hours post fertilization
ID	Intellectual disability

KCl	Potassium chloride
M	molar
MEF2	Myocyte-specific enhancer factor 2
MF20	atrial and ventricular meromyosin
MO	Morpholino-modified antisense oligonucleotide
mRNA	messenger RNA
l	liter
ml	milliliter
µg	microgram
µl	microliter
µM	micromole
mRNA	messenger RNA
PBS	Phosphate buffered saline
PCR	Polymerase chain reaction
PFA	Paraformaldehyde
PTU	Phenylthiourea
RNA	Ribonucleic acid
rpm	Rounds per minute
RT	Room temperature
SET domain	Domain first identified in 3 proteins Su(var)3-9, Enhancer of Zeste(z) and Trithorax of <i>drosophila elegans</i>
SETD5	SET domain-containing Protein 5
UV	Ultra violet
V	ventricle
vmhc	ventricular myosin heavy chain
WISH	Whole mount <i>in situ</i> hybridization
wt	wild-type

1 Introduction

1.1 Cardiovascular disease (CVD)

Every day, the human heart pumps approximately 7,200 liters of blood through its connected arteries and veins in order to constantly supply every single cell with oxygen and nutrients [18]. Therefore, the heart and the vascular system is indispensable for life. In 2016, cardiovascular diseases (CVDs) were the leading cause of death worldwide and were not only a burden to health but also to global economy [35].

CVD is a generic term framing all sorts of cardiac and vascular diseases. The World Health Organization differs between CVDs due to atherosclerosis and other CVDs such as cardiomyopathy, congenital heart disease and cardiac arrhythmia [3, 31, 35].

The “ideal cardiovascular health” is acquired by healthy lifestyle habits and defined through normal body weight, regular blood pressure levels, laboratory findings within normal limits, no drug treatment and no evident clinical manifestation of cardiovascular disease [35]. Although most factors leading to CVD are preventable, the pathogenesis highly depends on acquired or inherited disease generating genetic changes [7, 31]. In basic research, emphasis is put on different genetic mutations, since they can lead to perturbed cell signaling followed by dysfunction at cellular and tissue level [3]. In the past decades, suspected disease genes have been proven to drive cardiovascular disease generation and progression. Lately, cardiovascular research does not only focus on disturbed transcription and translation of CVD candidate genes, in fact disturbances in epigenetic transcription regulation were found to play a key role in CVD [3].

1.2 Epigenetic regulation of gene expression in cardiovascular disease

Multicellular organisms share the same genetic material in each cell. Nevertheless, cell-phenotypes are not identical. Differentiation of cell types can

evolve due to variation in chromatin modification, the so-called epigenome [38]. Different epigenetic mechanisms can modulate gene activity by generating a repressive heterochromatic state or an open euchromatic conformation of the genome, allowing gene transcription [38, 47]. As a matter of fact, more than 60% of the mammalian genome is permanently silenced by DNA methylation or histone modification [19].

The histone code hypothesis states, that patterns of post-translational histone modification give rise to distinct states of chromatin, which regulate DNA-accessibility to the transcriptional machinery [6]. Side chains of amino acids of free histone tails outside of the nucleosome are covalently modified through acetylation, methylation, phosphorylation, ubiquitination and sumoylation [8, 55, 62]. Depending on the site within the histone tail, the number of groups added and the region of chromatin, posttranslational histone modifications can either be activating or repressing [3].

Heart physiology, heart development and CVD are known to be highly dependent on dynamic chromatin remodeling, although the specific underlying mechanisms are still subject of investigation [49]. The most extensively studied effect of chromatin modifiers in the heart, is the role of histone deacetyltransferases (HDACs) [11, 49, 66]. HDACs are essential players to balance cardiac proteostasis, while impairments lead to cardiac hypertrophy, cardiomyopathy and atrial fibrillation [65, 66]. Histone tail acetylation is known to activate transcription by providing a non-compact euchromatic state, thereby influencing the transcriptome of the cell [11, 49].

Understanding the interaction of chromatin modifications and gene expression in CVD pathogenesis is still challenging, but inevitable to increase our knowledge of basic biology and to develop novel therapeutics [3].

1.3 The family of SET domain-containing proteins

Besides chromatin acetylation, histone methylation also plays an important role in epigenetic regulation of chromatin accessibility. Histone methyltransferases (HMT) methylate lysine residues on histone tails by adding one, two or three methyl-groups. Methylation by HMTs is not exclusively restricted to histones, other non-

histone proteins can also be methylated [8, 11]. Context and event of methylation determine whether transcription is being activated or repressed [11].

Most of the lysine-residue-methyltransferases share an evolutionary conserved SET domain [8, 55]. This SET (*Su(var)3-9*, *E(z)* and *Trx*) domain comprising approximately 130 amino acids was first identified as a conserved region in three groups of chromatin regulating proteins in *Drosophila melanogaster*, namely suppressor of variegation 3-9 (*Su(var)3-9*), enhancer of zeste (*E(z)*) and the trithorax (*Trx*) [8, 19, 62].

To date, SET domain-containing proteins can be divided into ten subfamilies, although histone methyltransferase (HMT) activity is not reported for all known SET containing-proteins [55]. Some SET domain-containing proteins have shown to be inevitable for cardiac muscle development. For example, the MYND and SET domain-containing protein *Bop* mediates ventricular cardiomyocyte maturation through chromatin modification [12]. *Smyd1b*, also a member of the SET domain family, is indispensable for cardiac myofibrillogenesis [40].

1.4 SET domain-containing protein 5

Different SET domain-containing proteins have been identified in various organisms. In zebrafish (*danio rerio*), 58 SET domain-containing genes have been identified so far [55]. One of those genes is the SET domain-containing protein 5 gene (*setd5*) [55]. Together with mixed-linkage leukemia 5 (*mlf5*), *setd5* belongs to subfamily VIII of the SET domain group of chromatin modifiers and has to date not been found to function as a histone methyltransferase [55].

However, detailed information concerning the expression pattern and function of *SETD5* in vertebrates is still an object of investigation. Studies of intellectual disability (ID) in humans revealed that 0.7% of the patients with ID share a *SETD5* mutation [13, 23]. Some of the patients with an alteration in *SETD5* suffered from congenital heart defects, mainly atrial and ventricular septal defects [13, 23, 56]. Osipovich *et al.* introduced a *Setd5* mouse knockout model, showing that mouse embryos die at E 10.5 prior to birth due to cardiovascular defects [39]. Thus, effects of *Setd5* mutation in mouse development after birth remain unstudied.

1.5 The zebrafish *danio rerio* – an ideal model organism to detect cardiac phenotypes

In the past 30 years, the tropical freshwater zebrafish (*danio rerio*) has emerged as a powerful model organism to study vertebrate biology and function [16, 46], filling the gap between invertebrates like flies and worms and higher vertebrates like mice and humans [2]. With the start of the sequencing project of the Wellcome Trust Sanger Institute in 2001, high quality zebrafish genome-sequence information has been available to scientists all over the world. The complete annotation of protein-coding zebrafish genes has made identification of human orthologues possible. As a matter of fact, for more than 70% of the human genes at least one distinct assignable zebrafish orthologue can be found [16]. Comparisons between humans and fish can be drawn not only because of their genetic homology, as vertebrates they also share common features from general anatomy and physiology to identical mechanisms in embryonic development. Humans and fish even share similar molecular pathways [16].

Focusing on molecular cardiology, the zebrafish has a closed cardiovascular system [7] and develops a two chambered heart with one atrium and one ventricle divided by the atrioventricular canal (AVC) [28]. Even though a mammal heart is composed of four chambers due to the need of a pulmonary circulation system, fundamental electrical properties of the cardiac conduction system of mammals and fish are identical [1, 7, 28, 53]. Heart rates of zebrafish (120-180bpm) and humans (60-120bpm) are easily comparable since ionic currents, action potential generation and QT interval duration closely resemble each other. By way of comparison, mice hearts beat 7 to 10 times faster than human hearts, also ionic currents and repolarization mechanisms differ strongly [1, 15, 46].

Danio rerio is not only a suitable model of human cardiology, but also easy and highly economic to raise and maintain. Zebrafish display high fecundity and a large amount of offspring, namely 200 to 300 eggs per single female fish per week [28, 46, 52]. The rapid ex-utero development of the transparent embryos can be studied by optical microscopy in a simple Petri dish and can be manipulated at any developmental stage [28, 53]. Already after 24 hours post-fertilization (hpf), the embryo has developed most primordial organs, including a contractile heart tube.

One day later at 72hpf, most internal organs comprising the heart have matured [46, 52].

For investigation of cardiac defects, zebrafish became the leading organism, since cardiac malformations do not affect the overall development of the embryo. Oxygen and nutrients demand of all tissues can be satisfied by passive diffusion in the first week of fish development [7, 52]. Therefore, the zebrafish is a very powerful model organism to investigate cardiovascular disease.

1.6 Forward and reverse genetics in zebrafish

With the model organism zebrafish, large scale genetic screens have become possible. One screening approach called forward genetics aims to determine the genetic basis responsible for a certain phenotype [7, 46]. Genome alteration can be achieved using for example ethylnitrosurea (ENU) to generate a great range of mutant phenotypes [2, 7, 54]. Mutations appear randomly in the fish genome, so the mutation localization causing a certain phenotype is the object of investigation [7, 54].

Another approach, the so called reverse genetics starts at the base of a certain genotype and investigates the induced phenotype. Targeted gene inactivation is needed to create specific genotypes for reverse genetics. One tool used for targeted gene inactivation is utilizing designed Morpholino-modified antisense oligonucleotides (Morpholinos) which are injected into fish embryos at one-cell stage. The induced phenotype can be investigated at any desired embryonic age, giving a fast and powerful tool to dissect molecular pathways of development and disease generation [9]. Depending on their design, Morpholinos inhibit translation or affect splicing in all embryonic to larvae stages (100-120hpf) when the duration of Morpholino effectiveness decreases [28, 52, 59].

With the help of the recently discovered clustered regularly interspaced short palindromic repeats (CRISPR)-Cas9 endonuclease system, the zebrafish genome can be specifically and permanently altered, making reverse genetics even more precise and stable [27, 29].

With the ease of genetic modification, *danio rerio* has emerged as powerful model organism to study human disease.

1.7 Aim of work

Mutations of the SET domain-containing protein 5 (*Setd5*) have been previously connected to intellectual disability and congenital heart defects in humans. Furthermore, experiments in mice showed that deletion of *setd5* is embryonic lethal because of defects in the developing cardiovascular system [39].

Besides the connection to cardiovascular diseases in mice and humans, not much more is known about the functions of *setd5*. Since the loss of *Setd5* leads to death during the embryonic development in mice, the zebrafish was chosen as a model organism, because of its ease of genetic manipulation and the ability to survive without a functional cardiovascular system.

The purpose of the present study was to characterize the function of *setd5* by knockdown studies *in vivo*, emphasizing cardiac phenotypes. Therefore, analysis of protein localization and gene expression at different developmental stages provided a temporal and spatial expression pattern of *setd5*. Cardiomyocyte differentiation and specification were evaluated to check for defects in early heart development due to the loss of *setd5*. Experiments on heart morphology were performed to visualize structural alterations in hearts lacking *setd5*. Additional investigations of heartbeat and contractility evaluated the functional defects after knockdown. Furthermore, chromatin modification analysis has revealed a possible influence of *setd5* on the chromatin state.

2 Material and Methods

2.1 Material

2.1.1 Technical Equipment

The used laboratory and technical equipment is alphabetically listed below.

BioDoc Analyze/ UV Star Biometra GmbH;
Göttingen, Germany

Cameras

Axiocam MRc Carl Zeiss AG;
Oberkochen, Germany

Leica DFC400 Leica Microsystems GmbH;
Wetzlar, Germany

Olympus DP72 Olympus Europa SE & CO. KG;
Hamburg, Germany

Proxitronic EL 4 S/N: 0269 ProxiVision GmbH;
Bensheim, Germany

Capillary puller PC-10 Narishige CO. Ltd.;
Tokyo, Japan

Centrifuges

Refrigerated centrifuge 5415 R Eppendorf AG;
Hamburg, Germany

Refrigerated centrifuge 5418 Eppendorf AG;
Hamburg, Germany

Electroporator micropulser BIORAD Laboratories GmbH;
Munich, Germany

Gel combs and chambers PeqLab, VWR;
Erlangen, Germany

Image Quant LAS 4000 mini GE Healthcare Life Sciences;
Freiburg, Germany

Material and Methods

Incubators

B6200, B6120 (fish), TypB12 (bacteria)	Thermo Fisher Scientific Germany BV & Co KG; Braunschweig, Germany
Injection apparatus FemtoJet	Eppendorf AG; Hamburg, Germany
Magnetic stirrer RCT basic	IKA®-Werke GmbH & Co. KG; Staufen, Germany
Manipulator M-152	NARISHIGE Co. LTD; Willow Way, London, United Kingdom

Microscopes

Axioskop2 plus	Carl Zeiss AG; Oberkochen, Germany
Electron microscope JEM-1400	Jeol GmbH; Freising, Germany
iMIC Digital microscope	KEYENCE Deutschland GmbH; Neu-Isenburg, Germany
Leica DM IL LED	Leica Microsystems GmbH; Wetzlar, Germany
Leica TCS SP8	Leica Microsystems GmbH; Wetzlar, Germany
Olympus SZX16	Olympus Europa SE & CO. KG; Hamburg, Germany
Zeiss Axio V.16	Carl Zeiss AG; Oberkochen, Germany
Microtome RM2145	Leica Microsystems GmbH; Wetzlar, Germany
PCR Mastercycler Pro	Eppendorf AG; Hamburg, Germany

Material and Methods

Photometer BioPhotometer	Eppendorf AG; Hamburg, Germany
Pipettes Research plus	Eppendorf AG; Hamburg, Germany
Power supply PEG Power 300	PeqLab, VWR; Erlangen, Germany
Refrigerators and freezers	Liebherr; Biberach a.d. Riß, Germany
Rocking incubator	Thermo Fisher Scientific Germany BV & Co KG; Braunschweig, Germany

Rocking platforms

Duomax 1030	Heidolph Instruments GmbH & Co. KG; Schwabach, Germany
Multi Bio 3D	Biosan; Riga, Lettland

Scales

Precision scale ED124S	Sartorius AG; Göttingen, Germany
Scale Adventurer	OHAUS Europe GmbH; Nänikon, Schweiz
Spectrophotometer NanoDrop 2000	Thermo Fisher Scientific Germany BV & Co KG; Braunschweig, Germany
Thermomixer comfort	Eppendorf AG; Hamburg, Germany

UV lamp

HXO 120V	Leistungselektronik Jena GmbH; Jena, Germany
Leica EL6000	Leica Microsystems GmbH; Wetzlar, Germany

Material and Methods

X-cite Series 120Q	EXFO Inc.; Unterhaching, Germany
UV light table BioDoc analyzer	Biometra GmbH; Göttingen, Germany
Vortex genie 2	Scientific Industries Inc.; New York, USA

2.1.2 Consumables

All consumables that were used in course of this work were put in alphabetical order.

Amersham ECL Prime	GE Healthcare Life Sciences; Freiburg, Germany
Bradford Protein assay	Bio-Rad Laboratories GmbH; Munich, Germany
Cell culture 4/8-well cover slides	SPL Life Sciences Co.; Naechon-Myeon, Pocheon-si, Korea
CELLSTAR® cell culture dishes (75 cm ²)	Sigma-Aldrich Co. LLC; St. Louis, USA
Cuvettes	ratiolab GmbH; Dreieich, Germany
Electroporation cuvettes	Bio-Rad Laboratories GmbH; Munich, Germany
Eppendorf Tubes	Eppendorf AG; Hamburg, Germany
Falcons	Becton Dickinson GmbH; Heidelberg, Germany
Fish food	
Artemia eggs	Sanders Brine Shrimp Co.; Utah, USA
Fish food (dry)	Tetra GmbH;

Material and Methods

	Melle, Germany
Fish food Gemma Micro	Skretting; Stavanger, Norway
Forceps	NeoLab Migge Laborbedarf-Vertriebs GmbH; Heidelberg, Germany
GeneRuler DNA Ladder Mix	Thermo Fisher Scientific Germany BV & Co. KG; Braunschweig, Germany
Glass capillaries	World Precision Instruments; Sarasota, USA
ImmEDGE™ pen Hydrophobic Barrier Pen	Vector laboratories INC; Burlingame, USA
Lipofectamin 2000 Transfection Reagent	Thermo Fisher Scientific Germany BV & Co. KG; Braunschweig, Germany
Matrices for injection ramp	Eppendorf AG; Hamburg, Germany
Microloader	Eppendorf AG; Hamburg, Germany
Microscope slides with depression	Thermo Fisher Scientific Germany BV & Co. KG; Braunschweig, Germany
Microscope slides without depression	Thermo Fisher Scientific Germany BV & Co. KG; Braunschweig, Germany
NBT/BCIP Stock Solution	Roche Diagnostics GmbH; Mannheim, Germany
PageRuler™ Prestained Protein Ladder	Thermo Fisher Scientific Germany BV & Co. KG; Braunschweig, Germany
Pasteur pipettes glass	VWR International GmbH; Darmstadt, Germany
Pasteur pipettes plastic	Brand GmbH & Co. KG; Wertheim, Germany

Material and Methods

Petri dishes	Greiner Bio-One International GmbH; Kremsmünster, Austria
Pipette tips	Brand GmbH & Co. KG; Wertheim, Germany
Preparation needles	NeoLab Migge Laborbedarf-Vertriebs GmbH; Heidelberg, Germany
Red sea salt	Red Sea Deutschland; Düsseldorf, Germany
Scalpels	B. Braun Melsungen AG; Melsungen, Germany
Mini-PROTEAN®TGX™	Bio-Rad Laboratories, Inc;
SDS gel	Hercules, USA
Sterile filter	Merck KGaA; Darmstadt, Germany
Syringes 1ml; 50 ml (plastic)	Becton Dickinson GmbH; Heidelberg, Germany

2.1.3 Kits

Within the scope of this work, following kits were used according to manufacturer's instructions.

Gateway® BP Clonase® Enzyme Mix	Thermo Fisher Scientific Germany BV & Co. KG; Braunschweig, Germany
Gateway® LR Clonase® Enzyme Mix	Thermo Fisher Scientific Germany BV & Co. KG; Braunschweig, Germany
Gateway® LR II plus enzyme	Thermo Fisher Scientific Germany BV & Co. KG; Braunschweig, Germany
GeneElute HP Plasmid MiniPrep Kit	Sigma-Aldrich Co. LLC; St. Louis, USA
JB-4 Embedding Kit	Polysciences Europe GmbH; Eppelheim, Germany

Material and Methods

mMESSAGE mMACHINE® SP6/T7 Transcription Kit	Thermo Fisher Scientific Germany BV & Co. KG; Braunschweig, Germany
Pierce™ Primary Cardiomyocyte Isolation Kit	Thermo Fisher Scientific Germany BV & Co. KG; Braunschweig, Germany
QIAprep Spin Miniprep Kit	QIAGEN GmbH; Hilden, Germany
QIAquick Gel Extraction Kit	QIAGEN GmbH; Hilden, Germany
QIAGEN Plasmid Maxi Kit	QIAGEN GmbH; Hilden, Germany
RNeasy Mini Kit	QIAGEN GmbH; Hilden, Germany
SuperScript® III Reverse Transcriptase	Thermo Fisher Scientific Germany BV & Co. KG; Braunschweig, Germany
TOPO® TA Cloning® Kit, Dual	Thermo Fisher Scientific Germany BV & Co. KG; Braunschweig, Germany
VECTASHIELD® Hard Set™ Mounting Medium with Dapi	Vector Laboratories Inc.; Burlingame, CA 94010

2.1.4 Plasmid backbones

Plasmid backbones used in course of this study were purchased from ThermoFisher Scientific Germany BV & Co. KG; Braunschweig, Germany (Invitrogen) or Addgene, LCS Standards Teddington, UK.

pCRII-TOPO-TA	<i>in situ</i> probe cloning,
pDESTcsII-myc	Gateway Cloning and mRNA synthesis,
pDestTol2pA2	MultiSite Gateway Cloning [24]
pDONR211/pDONRzeo	Gateway Cloning,
p5E-CMV	MultiSite Gateway Cloning [24]
p5E-MCS	MultiSite Gateway Cloning [24]

2.1.5 Restriction Enzymes

All Restriction Enzymes were purchased from NEW ENGLAND BioLabs and used according to the manufacturer's instructions.

2.1.6 Bacteria strains

One Shot® TOP10 Competent Cells *E. coli* were used produced by ThermoFisher Scientific Germany BV & Co. KG; Braunschweig, Germany.

2.1.7 Chemical reagents

Chemical reagents were acquired by Amersham, AppliChem, Braun, Fluka, Invitrogen, Lonza, Merck, NEW ENGLAND BioLabs, Polysciences, QIAGEN, Roche, ROTH, SIGMA-ALDRICH, Stratagene and VWR. Purified water was purchased from BRAUN, hereafter termed as ddH₂O.

2.1.8 Buffers and working solutions

All buffers and solutions are alphabetically listed below and were prepared according the following instructions.

Blocking buffer 1 (cell culture)	1 % BSA powder in PBS
Blocking buffer 2 (MF20/S46)	10% FCS in PBDT
Blocking buffer 3 (MF20/S46)	1.5% FCS in PBDT
Blocking buffer 4 (<i>in situ</i> hybridization)	2 mg/ml BSA in PBT; 5 % sheep serum
Blocking buffer 5 (<i>in situ</i> hybridization)	2 mg/ml BSA in PBT
Blocking buffer 6	5% not fat milk powder in TBST

Material and Methods

(Western blot)	
Blocking buffer 7 (Western blot)	5 % milk powder; 1 % BSA powder in TBS
Blocking buffer 8 (Western blot)	5% BSA in TBST
10x Blotting buffer (Western blot)	3.2 g Tris 144 g Glycin ad 1 l ddH ₂ O
1x Blotting buffer (Western blot)	150 ml methanol 100 ml 10x Blotting buffer ad 1 l ddH ₂ O
Deyolking buffer (Western blot)	55 mM NaCl 1.8 mM KCl 1.25 mM NaHCO ₃
E3 buffer (embryo media)	5 mM NaCl 0.17 mM KCl 0.33 mM CaCl ₂ 0.33 mM MgSO ₄
Hybridization buffer (<i>in situ</i> hybridization)	50 % Formamid 25 % 20x SSC 5 mg/ml torula RNA 50 µg/ml Heparin 0.1 % Tween 20
Infiltration solution A (JB-4 embedding)	100 ml JB-4 Embedding Solution A (Monomer) 1.25 g Benzoyl Peroxidase Plasticized (Catalyst)
Infiltration solution B (JB-4 embedding)	25 ml Infiltration Solution A 1 ml JB-4 Embedding Solution B
3x Laemmli-buffer (Western blot)	2.4 ml 1 M Tris HCl (pH 6.8) 3 ml 20 % SDS

Material and Methods

	3 ml Glycerol (100 %)
	1.6 mL beta-Mercaptoethanol
	0.006 g Bromphenol Blue
	ad ddH ₂ O to the total volume of 1l
LB-Agar (bacteria)	30 g LB-Agar ad 1l ddH ₂ O
LB-Medium (bacteria)	20 g LB-Broth ad 1l ddH ₂ O
Loading Dye (agarose) (electrophoresis)	0.25 % Xylencyanol 0.25 % Bromphenol blue 30 % Glycerol
Lysis buffer	10 mM Tris-HCl (pH 8.3) 50 mM KCl 0.3 % Tween 20 0.3 % Nonidet-P40
MESAB	4 mg/ml Ethyl-m-Amino-benzoat- Methanesulphonat 1 % Na ₂ HPO ₄ pH 7.0-7.5
2.5 % Methylcellulose	1.25 g Methylcellulosis in 50 ml E3
NTMT (<i>in situ</i> hybridization)	M Tris-HCl; pH 9.5 50 mM MgCl ₂ 0.1 M NaCl 0.1% Tween 20
PBDT	1% DMSO in PBT
PBS	137 mM NaCl 2.68 mM KCl 10 mM Na ₂ HPO ₄ 1.8 mM KH ₂ PO ₄ pH 7.4

Material and Methods

PBT	0.1% Tween 20 in 1 x PBS
4% PFA in PBS (fixation)	4% Paraformaldehyde in PBS for solving add 0.1 M NaCl and heat up to 68°C
100x PTU	20 mM 1-Phenyl-2-Thiourea in E3
20x SSC (<i>in situ</i> hybridization)	3 M NaCl 0.3 M sodium citrat pH 7.0
Stock B	22.1 g NaHCO ₃ 6.1 g Na ₂ SO ₄ add 1l ddH ₂ O
10x TBE	121.1 g Tris 3.72 g EDTA 51.53 g Boric acid pH 8 (NaOH) ad 1l ddH ₂ O
TBS 20x	175.32 g NaCl 121.1 g Tris-Base ad 1l ddH ₂ O, pH 7.4
1x TBST	1x TBS 0.05% Tween-20
TNN-stock solution (Protein extraction)	5 ml 1 M Tris-Cl, pH7.5 12 ml 5 M NaCl 5 ml 0.5 M EDTA 25 ml 10 % NP-40 1.33 g Na ₄ P ₂ O ₇ 0.184 g Na ₃ VO ₄ 2.1 g NaF ad 500ml ddH ₂ O
TNN-Working buffer	TNN-stock solution

Material and Methods

(Protein extraction)	Proteinase Inhibitor stock solution (10x) 1:10 PMSF 1:100-1:1000 1mM Na ₃ VO ₄ 1mM NaF 1mM DTT
Washing buffer	10 mM NaCl
(Western blot)	3.5 mM KCl 27 mM CaCl ₂ 10 mM Tris/Cl, pH 8.5

2.1.9 DNA oligonucleotides

All oligonucleotides were purchased from Eurofins Genomics and dissolved in ddH₂O to a concentration of 50pmol/μl.

β-Actin_Fw	5'-GCAGAAGGAGATCACATCCCTGGC-3'
β-Actin_Rv	5'-CATTGCCGZCACCTTCACCGTTC-3'
Setd5_Gateway_Fw	5'-GGGGACAAGTTTGTACAAAAAAGCAGGC TCTATGAGCATAGTAATCACACTGGGAG-3'
Setd5_GatewayStop_Rv	5'-GGGGACCACTTTGTACAAGAAAGCTGGG TCCTAAAAGCTGCCCGACTGTG-3'
Setd5_GatewayNoStop_Rv	5'-GGGGACCACTTTGTACAAGAAAGCTGGG TCAAAGCTGCCCGACTGTGT-3'
Setd5_ISH_F2	5'-TCTGCGTCAGAGACCAGTGT-3'
Setd5_ISH_R2	5'-CAGTGTTGTTGCAAGCCAGT-3'
Setd5_Splice_F1	5'-CAGCAGTTTGAAGTCAACGGAC-3'
Setd5_Splice_R2	5'-GGTTTGGTGTAGTGCTCCATTC-3'

2.1.10 Antibodies

Antibodies used in this work are alphabetically listed below.

2.1.10.1 Primary antibodies

mouse-anti- β -actin	1:2000	Sigma-Aldrich #A5441
mouse-anti- β -catenin	1:	Sigma-Aldrich #C7207
mouse-anti-MF20	1:10	Hybridoma Bank P3U-1 myeloma cell line
mouse-anti-S46	1:50	Hybridoma Bank P3/NS 1.1Ag4-1
rabbit-anti-Acetylated- Histone 4	1:2000	Abcam ab177790
rabbit-anti-GFP	1:200	Invitrogen #A11122
rabbit-anti-MEF2	1:200	Santa Cruz sc-313
rabbit-anti-Methylated- Lysine	1:3000	Abcam ab23366
rabbit-anti-pan-cadherin	1:50000	Abcam ab16505
Rabbit-anti-Pan- Methylated-Histone3 (Lys9)	1:3000	Cell Signaling #4069S
rabbit-anti-Setd5-1 (N-term)	1:100	Aviva Systems Biology ARP49310_P050
rabbit-anti-Setd5-2 (polyclonal)	1:100	Cohesions Bioscience limited CQA1566

Material and Methods

2.1.10.2 Secondary antibodies

goat anti-mouse IgG1 (Alexa Fluor 488)	1:1000	Invitrogen #A21121
goat anti-mouse IgG1 (Alexa Fluor 555)	1:1000	Invitrogen #A21127
goat anti-mouse IgG2b (Alexa Fluor 488)	1:1000	Invitrogen #A21141
goat anti-mouse IgG2b (Alexa Fluor 555)	1:1000	Invitrogen #A21147
goat anti-rabbit IgG (Alexa Fluor 488)	1:1000	Invitrogen #A32731
goat anti-rabbit IgG (Alexa Fluor 555)	1:1000	Invitrogen #A21429

2.1.11 Fluorescence Dye

Calcium Green-1 dextran (C37139) was purchased by ThermoFisher Scientific Germany BV & Co. KG; Braunschweig, Germany.

2.1.12 Morpholino modified antisense oligonucleotides (MO)

All Morpholino modified antisense oligonucleotides were directed against *setd5* (NCBI: ID 570278) and purchased from Gene Tools; LLC, Oregon, USA.

Gene	Target	MO sequence 5'- 3'	Name
<i>setd5</i>	Exon10-Intron11 boundary	AGCTTCAACATATTGGTCTCACCTC	MO1- <i>setd5</i>
	E10I11-5bp- mismatch	AGgTTgAAgATATTGcTgTCACCTC	MO1- <i>ctrl</i>
	Start-ATG	AGTGTGATTACTATGCTCATGACGT	MO2- <i>setd5</i>
	Start-ATG-5bp- mismatch	AGTcTcATTAgTATcCTCATcACGT	MO2- <i>ctrl</i>

Material and Methods

2.1.13 Fish lines

The following fish lines were used for the accomplished experiments:

TE	wild-type line
<i>flatline</i>	mutation within the <i>smyd1b</i> gene; <i>smyd1b</i> ^{zf340/zf340} [26]
<i>Tg(fli:eGFP)</i>	Transgenic line, using the fli-promotor to express enhanced green fluorescent protein [25, 45]

2.1.14 Software

ApE v2.0.37	A plasmid Editor by M. Wayne Davis
Axio Vision SE64 V4.9.1.0	Carl Zeiss Microscopy GmbH
CellSens Entry 1.5	Olympus Corporation
EndNote X7	Thomson Reuters
Image J 1.51h	Wayne Rasband, Nation Institute of Health, USA
Image Quant LAS 4000	G&E Healthcare Life Science
Leica application Suite LAS V3.7	Leica Microsystems (Switzerland) Limited
Microsoft Office 2016	Microsoft Corporation
Photoshop	Adobe Systems Incorporated
Prism 6	GraphPad
Ulead Video Studio	Corel VideoStudio

2.1.15 Databases/ Tools

Clustal Omega	http://www.ebi.ac.uk/Tools/msa/clustalo/
Ensemble	http://www.ensembl.org/index.html
ExpASy	http://www.expasy.org

Material and Methods

NCBI	http://www.ncbi.nlm.nih.gov/
OligoPerfect™	https://tools.thermofisher.com/
UniProt	http://www.uniprot.org/
ZFIN	http://zfin.org/

2.1.16 Statistics

The data were analyzed using Microsoft Office Excel and GraphPad Prism6. All results are expressed as means \pm standard derivation (SD). To calculate the significance of difference for the obtained data sets, first the data distribution was estimated by the D'Agosino and Shapiro-Wilk normality test.

In case of a Gaussian data distribution, the data sets were compared with the t-test. If the data sets did not pass the normality test, the data were compared with the Mann-Whitney test.

2.2 Methods

2.2.1 Alignment

The latest SETD5 protein sequences were provided by the National Center for Biotechnology Information (NCBI) protein database. NCBI Reference Sequences NP_001073986.1 (*homo sapiens*), NP_082661.1 (*mus musculus*) and XP_698834.4 (*danio rerio*) were used. Multiple sequence alignment was performed using Clustal Omega. Boxshade by ExPASy visualized chemical protein properties.

2.2.2 Zebrafish breeding and husbandry

Zebrafish breeding and husbandry were carried out mainly as described in “The Zebrafish Book - A guide for the laboratory use of zebrafish (*Danio rerio*)” [61]. The fish facility in Ulm built by Aqua Schwarz Aquarienbau housed the adult zebrafish in a rack system and contained a total volume of 10m³ deionized water at the constant temperature of 28°C. Daily automatic monitoring tested levels of nitrite, nitrate and ammonium levels in the water, including pH, conductivity and

Material and Methods

temperature. To simulate the natural habitat, the day night rhythm, with 11h darkness was kept constant as well. Fish were fed twice a day with either artemia eggs or dry food.

At the age of 3 months, zebrafish become fertile and can produce a sufficient amount of offspring. In the afternoon, the fish were separated by sex with the help of removable barriers in mating tanks. On the next morning, light served as a signal of copulation, therefore 15min after removing the separators, the offspring could be collected. The captured eggs were transferred to a petri dish and cultured in E3 medium.

2.2.3 Microinjection into zebrafish oocytes

Prior to microinjection, preparation of injection ramps was done, pouring melted 3% agarose in E3 into a petri dish. A casting mold containing 6 linear wells was placed on the surface of the warm agarose and removed after cooling. Injection needles were prepared by pulling 0.75mm capillaries with a capillary puller. The injection needles were carefully opened with the help of a razor blade and loaded with the desired substance (Morpholino or Calcium Green-1 dextran) using a micro loader. The fertilized eggs were collected, kept in E3 and transferred to the injection ramp using plastic Pasteur pipettes. The injection needle was inserted to the micromanipulator and connected to the FemtoJet microinjection device. Capillary pressure, injection pressure and injection time were adjusted according to the size of the needle tip opening. Microinjection was performed only during the one-cell stage when injecting Calcium Green-1 dextran into the cell and could be continued until the four-cell stage, when injecting Morpholino. The injected embryos were transferred to a Petri dish and kept in E3 under standard conditions at 28.5°C in the incubator. To prevent pigmentation development 250µl 1xPTU was added to E3 medium in each Petri dish not earlier than 24hpf. Phenotypes were examined by light microscopy and digital imaging at 24hpf, 48hpf and 72hpf.

2.2.4 Photo and Video documentation of zebrafish embryos

Depending on the developmental stage, embryos needed to be dechorionated manually with forceps, prior to photo- and video-documentation. Embryos were placed on a microscope slide with a depression filled with 2.5% methylcellulose

Material and Methods

and positioned with the help of a preparation needle. For photo documentation, a stereomicroscope by Olympus (Olympus SZX16) was used together with the provided CellSens Entry Software. Heart movies were recorded with an inverted stereomicroscope (Leica DM IL LED) using the Leica Application Suite software.

The same microscopes with an addition fluorescence lamp were used for fluorescence imaging.

Images of histological sections were taken by a Zeiss stereomicroscope (AxioSkop 2 plus) and documented in Axio Vision.

2.2.5 Functional measurements of heart rate and fractional shortening

Prior to functional measurements, embryos were adjusted to room temperature for at least 45min. For heart rates, embryos were embedded in 2.5% methylcellulose and heart contractions were counted in a 20sec interval. Multiplication by 3 resulted in the desired count of beats per minute (bpm).

Videos of 48hpf and 72hpf embryos were analyzed using ImageJ. Atrial and ventricular chamber diameters were measured at the end of contraction (systole) and the end of relaxation (diastole) and inserted in following formula to calculate fractional shortening (FS).

$$FS = \frac{\varnothing_{diastole} - \varnothing_{systole}}{\varnothing_{diastole}}$$

For each time point and group 5-10 embryos were used to determine heart rate and fractional shortening.

2.2.6 Calcium Imaging

Calcium Green-1 Dextran (200 μ M) was coinjected with MO1-*ctrl* or MO1-*setd5* (200 μ M) into *flatline* embryos at the one-cell stage. At 72hpf embryos were adjusted to room temperature and embedded in 2.5% Methylcellulose in the depression of the microscopy slide. Videos were taken by Proxitronic camera (Provision) at 29.97 frames per second and processed by Ulead Video Studio Software. Relative fluorescence measurements were done using ImageJ. A small box was selected in either atrium or ventricle to plot the z-axis profile. Graphic representation was done using Prism.

2.2.7 mRNA extraction from zebrafish embryos

To analyze gene expression of certain genes of interest, mRNA extraction of embryos at specific points of time is needed.

Embryos were collected, cleaned from expandable E3, put in liquid nitrogen and stored at -80°C. mRNA extraction started with homogenization by adding 1ml of trizol to approximately 70 embryos in the laboratory hood. Embryos were drawn up and down multiple times through 23 gauge / 27 gauge needles into syringes. After homogenization and 5min incubation at room temperature, 200µl Chloroform was added and 15sec vortexed. Incubation took 3min at room temperature. Centrifugation followed at 12000rpm for 15min at 4°C. 500µl Isopropanol were added to the supernatant and incubated for 10min at room temperature to drive mRNA precipitation. A mRNA pellet was generated by another centrifugation step (12,000rpm, 10min, 4°C) and washed by adding 1ml 75% ethanol. Centrifugation (7,500rpm, 15min, 4°C) and removal of the supernatant result in a pellet of RNA, which needed to be dried for at least 2h at room temperature. 30µl of DEPC-water was used to resuspend the mRNA pellet. mRNA concentration was measured using a spectrophotometer (NanoDrop 2000, Thermo Fisher Scientific).

2.2.8 Reverse transcription

1µg mRNA was transcribed into complementary DNA (cDNA) using Superscript® III Reverse Transcriptase (Life Technologies), following the manufacturer's instructions.

2.2.9 Polymerase chain reaction (PCR)

To clone and amplify parts or the entire sequence of a gene of interest, polymerase chain reactions were performed. Taq Polymerase (NEB) (TOPO-TA/blunt cloning; standard PCR) or Q5® Hot Start High-Fidelity DNA Polymerase (NEB) (Gateway Cloning) were used according to the manufactures' instructions. The following thermocycling conditions were programmed:

Material and Methods

Initial Denaturation	98°C	30sec	
Denaturation	98°C	10sec	
Primer Annealing	50-70°C	20sec	25-35 cycles
Extension	72°C	30sec/kb	
Final Extension	72°C	2min	
Hold	4°C	∞	

For Gateway Cloning, a two-step thermocycling setting was used:

Initial Denaturation	98°C	30sec	
Denaturation	98°C	10sec	
Primer Annealing	50-70°C	20sec	4 cycles
Extension	72°C	30sec/kb	
Denaturation	98°C	10sec	
Primer Annealing	72°C	15sec	35 cycles
Extension	72°C	30sec/kb	
Final Extension	72°C	2min	
Hold	4°C	∞	

2.2.10 Expression PCR

Primer directed against β -actin and *setd5* traced were used on cDNA probes of wildtype fish at different developmental stages (12 somites, 18 somites, 24hpf, 32hpf, 48hpf, 72hpf). Primer pair *Setd5_ISH_F2/R2* was taken to detected the expression of *setd5*, whereas Primers directed against β -Actin served as a control.

2.2.11 Agarose gel electrophoresis

To separate DNA or RNA fragments amplified by PCR, agarose gel electrophoresis was used. 1 or 2% gels were prepared according to the predicted product length using agarose and 1xTBE. The solution was brought to the boil and cooled down on an electric stirrer. When the temperature reached approximately 40°C ethidium bromide was added, to visualize DNA fragments through intercalation. After gelation, samples were mixed 1:6 with 6x loading dye and loaded on the gel. 1kb DNA ladder was used as a standard. After running at

120mV for 1-2hours, the gel was either documented or corresponding DNA bands were cut out.

2.2.12 DNA gel extraction

For further cloning (TOPO-TA/bunt or Gateway cloning) or sequencing, the amplified PCR products were extracted from agarose gel using the QIAquick Gel Extraction Kit according to the manufacturer's instructions.

2.2.13 Cloning

TOPO-TA cloning following the manufacturer's manual was used for *in situ* probe generation. The protocol provided by the manufacturer of the gateway cloning system was used to generate fluorophore or myc tagged gene constructs. Amplificats of the gene of interest from cDNA with gateway overhangs were introduced to the Gateway cloning system [24]. For the BP and LR clonase reaction the vectors pDONRzeo and pDESTcslI-myc were used.

Multisite gateway cloning formed a plasmid, composed of a pDestTol2pA2 backbone, a 5' promotor-insert (*CMV* or *cmIc2* promotor sequence), middle insert (no-stop variant of the gene of interest), and the 3' tag (sequence of eGFP).

2.2.14 Plasmid DNA preparation

Plasmid DNA preparation was accomplished following the manufactures instructions by using the QIAprep Spin Miniprep Kit (Qiagen) or QIAGEN Plasmid Maxi Kit (Qiagen).

2.2.15 Splice assay

Splice assay was performed using cDNA generated from wildtype, MO1-*setd5* and MO-*ctrl* injected embryos at 48hpf. MO1-*setd5* is directed against the splice-site between exon 10 and intron 11. Therefore, primers were designed to enclose the splice boundaries from exon 9 to exon 13 to provide for all contingencies.

Primer forward: Setd5_Splice_F1: 5'-CAGCAGTTTGAAGTCAACGGAC-3'

Primer reverse: Setd5_Splice_R2: 5'-GGTTTGGTGTTAGTGCTCCATTC-3'

Material and Methods

The PCR-mix was prepared using the general protocol, stated in 2.2.9.

Initial Denaturation	94°C	5min	
Denaturation	94°C	50sec	
Primer Annealing	58°C	50sec	50 cycles
Extension	72°C	1min	
Final Extension	72°C	10min	
Hold	4°C	∞	

2.2.16 Preparation of *in situ* probes

Generation of *in situ* probes of the gene of interest started with the amplification of a gene fragment of approximately 500bp in length, using Taq-PCR protocol and the TOPO-TA Cloning Kit. Restriction enzymes linearized the obtained plasmid for at least 2h. Precipitation was achieved by incubation in 7.5M ammonium acetate and ethanol (1:5) at -80°C for 30min. Thereafter, the linearized plasmid was pelletized in a centrifuge at 14,000rpm at 4°C for 15min and washed with 75% ethanol. The pellet was air dried and resuspended in 13µl ddH₂O. Transcription to mRNA was acquired using the mMESSAGE mMACHINE SP6 or T7 Transcription Kit according to the manufacturer's protocol. The probe was labeled with Digoxigenin. Afterwards, 24µl of the synthesized RNA was precipitated by adding 2.5µl LiCl (4 M) and 75µl 100 % ethanol and incubated at -80°C for 30min. Centrifugation at 14,000rpm at 4°C for 15min formed a pellet which was air-dried and resuspended in 50µl RNase free water. Finally, the *in situ* probe was diluted 1:100 in hybridization buffer for usage and stored at -80°C.

2.2.17 *In situ* hybridization

To determine the temporal and spatial expression of a gene of interest, whole mount *in situ* hybridization was performed as described before [58]. Instead of a 24-well plate described in the original protocol, all steps were performed in 2ml Eppendorf tubes.

2.2.18 Whole mount immunocytochemistry

For fixation purposes, collected embryos were kept in 4% PFA overnight and were then placed into 100% Methanol. The staining process started with rehydration steps in decreasing concentrations of Methanol in PBT (75:25; 50:50 and 25:75) for 20min each. Afterwards, the embryos were rinsed three times in PBDT. To prevent unspecific antibody binding, embryos were incubated in blocking buffer 2 (10% FCS/ PBDT) for at least 90min at room temperature. All followings steps were from now on performed at 4°C on a rocking platform. Embryos were incubated with MF20 primary antibody in blocking buffer 3 (1.5 % FCS in PBDT) (1:10) overnight. On the next morning four 30min-washing steps in blocking buffer 3 followed. The second primary antibody S46 was applied in a 1:50 dilution in blocking buffer 3 and incubated overnight. After the same four washing steps, the secondary antibodies were added to the embryos in a 1:100 dilution in blocking buffer 3 and kept under light protection until the next morning. Again, four washing steps followed and embryos were stored at 4°C in PBT protected from light until documentation.

2.2.19 JB4-Embedding and HE-staining

Embryos were collected in a 2ml tube and fixated in 4%PFA in PBS overnight. After rinsing them in PBT three times, the embryos were slowly dehydrated via increasing amounts of ethanol (1h each in 50%, 60%, 70%, 80%, 90% and 100% ethanol). Next, the embryos were incubated in 1ml JB-4 infiltration solution A at 4°C. On the next day, the solution was discharged, leaving the embryos in small amount of liquid. 1.5ml JB4-infiltration solution A and 60µl solution B were mixed in a 2ml tube with a plastic pipette until no streaks were visible and then added to the embryos. The volume was filled in an embedding mold and included embryos were positioned with a preparation needle. The block holder was carefully laid on top until polymerization was finished.

The embedded embryos were cut sagittally in 4-5µm sections using a microtome. The sections were placed on microscope slides and incubated for 10min in eosin. Eosin is an agent for staining alkaline and acidophilic cytoplasmic components. Next, slides were rinsed in water and then again stained, this time using

Hematoxylin, a marker staining acidic components of cell nuclei. After drying, the sections were ready for documentation.

2.2.20 Electron microscopy

At the electron microscope core facility in Ulm, employees first fixated (2.5% glutaraldehyde, 1% paraformaldehyde in 0.1M phosphate buffer, pH 7.3) the embryos at 48hpf, then they were post-fixated in 1% osmium tetroxide, dehydrated and embedded in Epon. Staff members also performed sectioning and ultrathin sectioning of the embedded embryos. Ultrathin sections (50 nm) were contrasted with uranyl acetate and lead citrate and examined on the electron microscope JEM-1400.

2.2.21 Protein extraction from zebrafish embryos

For Protein extraction, 50-100 whole zebrafish embryos were anesthetized, collected in a 1.5ml Eppendorf tube and immediately frozen using liquid nitrogen. Yolk sacks were removed by adding 1ml deyolking buffer to the tube and pipetting up and down, followed by vortexing for 15s. Centrifugation at 3,000rpm and 4°C for 30s formed a pellet. After removing the supernatant, two washing steps with 1ml washing buffer, 15s vortexing and 30s centrifugation at 3000rpm and 4°C followed. The pellet was resuspended in 75µl TNN working buffer and then homogenized with the help of a pestle under continuous freezing in liquid nitrogen. Thereafter, the probes were incubated for 15min on ice and then centrifuged at 4°C and 14,000 rpm for 10 min. The supernatant was finally transferred in a new 1.5ml Eppendorf tube, ready for Bradford protein concentration measurements and Western blotting.

2.2.22 Western Blot

For Western Blot analysis, 20µg of protein lysate in TNN was boiled in 3x Loading Dye (Laemmli buffer) and loaded on a precast 10% SDS gel (BioRad). Protein separation by SDS-PAGE was followed by protein transfer to a polyvinylidene fluoride (PVDF) membrane. Thereafter, the membrane was blocked in blocking buffer for at least 2h to saturate free binding sites on the membrane. Afterwards, the membrane was incubated with the primary antibodies at 4°C over night. The

next day, four washing steps in TBST for 15min at room temperature were followed by incubation with the secondary antibody for 2h at room temperature. Again, the membrane was rinsed four times in TBST. For development, Amersham ECL Prime was used according to the manufactures instructions and imaging was performed by luminescent image analyzer (Image Quant Las4000 mini).

2.2.23 Isolation and immunofluorescence staining of cardiomyocytes

From adult zebrafish, primary cardiomyocytes were isolated and cultured according to protocols in literature [51]. Neonatal mouse cardiomyocytes were isolated using the Pierce™ Primary Cardiomyocyte Isolation Kit by ThermoFisher Scientific according to the manufacturer's manual.

HEK293T human embryonic kidney cells were transfected with Tol2pA₂[CMV:setd5:eGFP] plasmid using Lipoflectamin 2000 Transfection Reagent (Invitrogen) following manufacturer's instructions.

For immunostaining, cells were first fixated in 3.7% formaldehyde for 15min at room temperature. After two washing steps in PBS, the cells were permeabilized for 5min in 0.5% Triton X-100 in PBS. Another 2 washing steps in PBS followed before blocking for 1h in 1%BSA in PBS to prevent unspecific antibody binding. Cells were washed twice in PBS and then incubated with the primary antibody (Setd5-1, Setd5-2 and β -Catenin) in 1%BSA/PBS overnight at 4°C. The next day, same two washing steps followed prior to incubation with the secondary antibody in 1% BSA/PBS overnight at 4°C. Cells were rinsed twice in PBS, before VECTASHIELD® Hard Set™ Mounting Medium with DAPI was applied to mount the samples. The slides were covered with a cover slide and ready for imaging at the Leica TCS SP8 microscope.

2.2.24 Heart Dissection

A humidified chamber and microscopic slides were prepared. Each slide was divided into eight small chambers using an immEDGE™ pen and filled with 50 μ l formaldehyde. Injected embryos at 72hpf were anesthetized with MESAB for 1min. Heart dissection was performed as described in literature [64]. Briefly, with the

Material and Methods

sharp edges of syringe needles, the heart was extracted and transferred to the prepared slide. From now on, all steps are performed on a rocking platform and not more than 50 μ l of volume are used. After incubation for 20min, the formaldehyde was removed and the two washing steps with PBST, each 5min, at room temperature followed. Probes were first blocked 60min in 10% sheep serum in PBT and then incubated with the primary antibody MEF2 in a 1:200 dilution at 4°C over night. On the next day, another three washing steps in PBST for 5min at room temperature followed, before incubation with the secondary antibody (1:1,000) for 30min at room temperature. After another three washing steps in PBST, all the liquid was removed, 10 μ l VECTASHIELD® Hard Set™ Mounting Medium with DAPI was applied and the entire slide was covered with a cover slide. Stored at 4°C, the dissected hearts could be kept until imaging at the iMIC Digital Microscope.

3 Results

3.1 *SETD5* is conserved among species

For the first time, the model organism *danio rerio* was introduced as a new approach to functionally characterize *setd5 in vivo*.

To investigate if *setd5* is evolutionarily conserved and to ensure that comparisons can be drawn between the three species *homo sapiens*, *mus musculus* and *danio rerio*, an amino acid sequence alignment was performed (Figure 1). Protein sequences were obtained from the National Center for Biotechnology Information (NCBI) protein database, which are retrievable under the following Reference Sequences: NP_001073986.1 (*homo sapiens*), NP_082661.1 (*mus musculus*) and XP_698834.4 (*danio rerio*). The highest degree of comparability was achieved by selecting SETD5 protein isoform 1 of each species.

Murine SETD5 demonstrated 94.24% sequence homology to its human orthologue, whereas the zebrafish sequence showed 49.06% homology to the human protein. By taking only the functional part of the protein, the conserved SET domain demonstrated high cross species homology. The zebrafish SET domain of the *setd5*-transcript shared 88.99% sequence identity to its human and murine orthologues, who presented 100% sequence identity (Figure 1, red box).

The alignment showed that the SET domain of *setd5* is evolutionary highly conserved among species, suggesting important biological functions *in vivo*.

Results

hs_SETD5	1	MSIAIPLGVTTSDTSYSDMAAGSDPESVEASPAVNEKSVYTHNYGTTQRHGCRGLPYATIIPRS-----DLNGLPSPV-----
mm_SETD5	1	MSIAIPLGVTTSDTSYSDMAAGSDPESVEASPAVNEKSVYTHNYGTTQRHGCRGLPYATIIPRS-----DLNGLPSPV-----
dr_SETD5	1	MSIVITLGVTTPTPTFYIDMAAGSDPESVEASPAVNEKN-YSSRSCGNTQSHCYGGLPYAQQSSVVCQDHNYSAPPEPTPPASPISQVTV
hs_SETD5	75	-----EERCQDPSNSEGETVPTWCPCGLSQDGFLLNCDKCRGMSRGKVI RLHRRKQDNISGGDSSAT
mm_SETD5	75	-----EERCQDPSNSEGETVPTWCPCGLSQDGFLLNCDKCRGMSRGKVI RLHRRKQDNISGGDSSAT
dr_SETD5	90	FSHAERNRTLGRSRPCFSTNEPNSADSSESEEEVVEGAIPPSWCSCHLNQDGFLLKCNCRGLEKPKKGVGDRKRAKINVSIVGSSSAT
hs_SETD5	137	ESWDEELSPSTVLYTATQHTPTTSITLTVRRTKPK---KRRKKSPEKGRAAPKTK-----KIKNSPSEAQNLDENTTEGWENRI
mm_SETD5	137	ESWDEELSPSTVLYTATQHTPTTSITLTVRRTKPK---KRRKKSPEKGRAAPKTK-----KIKNSPSEAQNLDENTTEGWENRI
dr_SETD5	180	ESGDEEMASAVSYTATQHTPTTSITLTVRRTKPKVHNKVKKRRKKSSTKTKTRTTPKAKKVKAYREGSRKSMRKNKNSASETSVLDENTTEGWETRI
hs_SETD5	211	RLWTDQYEEAFTNQYSADVQNALEQHLHSKKEF-VGKFAILLDTINKTELACNNTVIGSQMQLQQLGRVTRVQKHKRI LRAARDLALDTLII
mm_SETD5	211	RLWTDQYEEAFTNQYSADVQNALEQHLHSKKEF-VGKFAILLDTINKTELACNNTVIGSQMQLQQLGRVTRVQKHKRI LRAARDLALDTLII
dr_SETD5	270	RWTDQYEEALANQYSADVQTLLEHYCANGTNSPSTVAIDTINKTELACNNTVIGSQMQLQQLGRVTRVQKHKRI LRAARSLDPTLLII
hs_SETD5	300	EYRGKVMRLRQQFEVNGHFFKKPYFVFLFYSKFNGVEMCVDARTFGNDARFIRRSCTPNAEVRHMIADGMIHLCIYAVSAITKDAEVTIAF
mm_SETD5	300	EYRGKVMRLRQQFEVNGHFFKKPYFVFLFYSKFNGVEMCVDARTFGNDARFIRRSCTPNAEVRHMIADGMIHLCIYAVSAITKDAEVTIAF
dr_SETD5	360	EYRGKVMRLRQQFEVNGHFFKKPYFVFLFYSKFNEVEMCVDARTFGNDARFIRRSCTPNAEVRHMIADGMIHLCIYAVSAITKDAEVTIAF
hs_SETD5	390	DYEYSNENYKVDCACHKGNRNCPIQKRNPAEELPLPPPPSPPTI GAETRRRRKARRKELEEQONEVPEENPPEOEVPEKVTVSSNHH
mm_SETD5	390	DYEYSNENYKVDCACHKGNRNCPIQKRNPAEELPLPPPPSPPTI GAETRRRRKARRKELEEQONEVPEENPPEOEVPEKVTVSSNHH
dr_SETD5	450	DYEFSCENYKVDCACHKGNQDCPQVQHNLRPEELLSQEQEALPAGAEFRRRRARRRELEGLKLVTSISESHLLELGNFAHGSSDTE
hs_SETD5	480	EEVDNPEEKPEEE-KEEVLDDQENLAHSRRTRREDRKYVAIMHAFENLEKRRKRRDQPEQSSSDVEITITTSSETPVGEETKTAAPSESVS
mm_SETD5	479	EEVDNPEEKPEEEKKBATDDQENS AHSRRTRREDRKYVAIMHAFENLEKRRKRRDQPEQSSSDVEITITTSSETPVGEETKTAAPSESVS
dr_SETD5	539	---DAIMNIVKLENGEBEIDENGALTPNRRSREERKKAIAIMHMFENLEKRRKRCQVTAQAIAEETKLE-----AGEAEVVP
hs_SETD5	569	NSVSNVITPSTPQSGVNTRRSSQ-----AGDVAEKLVPKPPPAKPSRPRPKSRI SRYRTSSAQRLLKROKQAAQQQAELSQAAL
mm_SETD5	569	SPVSNVAIPSTPQSGVNTRRSSH-----AGDVAEKLVPKPPPAKPSRPRPKSRI SRYRTSSAQRLLKROKQAAQQQAELSQAAL
dr_SETD5	611	SA--GNCPFNAAAAGVCTRSSFVTLDTADDSDSEKPTATPSPAPKQPARSKPRPKSRI SRYRTSSAQRARROKAAQQQAEVGVVVG
hs_SETD5	649	EEGGSNSLVTPEAGSLDSSGENRPLTGSDFPT-VISVTGSHVNRAASKYPKTKKYLVTWELNDKAD-KQECVPECPLRITTDPTVLAT
mm_SETD5	649	EEGGSNSLVTPEAGSLDSSGENRPLTGSDFPT-VISVTGSHVNRAASKYPKTKKYLVTWELNDKAD-KQECVPECPLRITTDPTVLAT
dr_SETD5	699	GEEGSAAAGL-KE----QGGGEGALNCHLQDGEYGAASGGMENKTHVHPKTKKYLVTWELNDKADKVERVESVERPLRITTDPTVLAT
hs_SETD5	735	TLNMLPGLIHSPLICTTPKHVIRFGSPFPERRRRRPLPDGTFSSCKKRWIKQALEEGMTQTSVSPQETRTOHLYQSNENSSSSSICKDN
mm_SETD5	735	TLNMLPGLIHSPLICTTPKHVIRFGSPFPERRRRRPLPDGTFSSCKKRWIKQALEEGMTQTSVSPQETRTOHLYQSNENSSSSSICKDN
dr_SETD5	784	TLNMLPGLIHSPLICTTPKHVIRFGSPFPERRRRRPLPDGTFSSCKKRWIKQALEEGMTQTSVSPQETRTOHLYQSNENSSSSSICKDN
hs_SETD5	825	ADLLSPLKWKKSRYLME---QNTKLLRPLSPVTPPPSSGSKSP--QLATPGSS--HPGEEECRNGYSLMFSPITSLTTASRCNTPLQFE
mm_SETD5	825	ADLLSPLKWKKSRYLME---QNTKLLRPLSPVTPPPSSGSKSP--QLATPGSS--HPGEEECRNGYSLMFSPITSLTTASRCNTPLQFE
dr_SETD5	872	PILLTCEFKKRLKCSSETAAPPSEL LRLPLSPITPLPESEYPIPLPLSLNPLCSLYLGEVEFKRNTVLSMSPITSLTTASRCNTPLQFE
hs_SETD5	909	LCHRKDLDLAKVGLDSDNTNSCAD-----RPSLLNCSGSDLAPHP-----SICPTSETGFPS-----RSGDGHQTLVRN
mm_SETD5	909	LCHRKDLDLAKVGLDSDNTNSCAD-----RPSLLNCSGSDLAPHP-----SICPTSETGFPS-----RSGDGHQTLVRN
dr_SETD5	961	NLSSPASPVHISESL-IPDPCLRSDFTSRVAFFPFDSTSRSEPAVSEDFSLPAPDSLNGSGGCTFRSSAVVSTLDCDSALVSHASETQT
hs_SETD5	973	SDQAFRTEFNLMYAYSPLNAMPRADGLYRGSPLVGDGRKPLHLDDGGYCSPAEGFSSRYEHGLMKDLRSGSLSPG-----GERACEGVPSAP
mm_SETD5	973	SDQAFRTEFNLMYAYSPLNAMPRADGLYRGSPLVGDGRKPLHLDDGGYCSPAEGFSSRYEHGLMKDLRSGSLSPG-----GERACEGVPSAP
dr_SETD5	1050	RQAFRTEFNLMYAYSPLNAMPRADGLYRGSPLVGDGRKPLHLDDGGYCSPAEGFSSRYEHGLMKDLRSGSLSPG-----GERACEGVPSAP
hs_SETD5	1058	QNPPQRKKVLSLEYRKRKQEAKEKNSAGGGGSDSAQSKSKSAGAGQGSSNSVSDTGAHGVQSSARTPSSPHKKFSPSHSSASHLEAVSPSD
mm_SETD5	1058	QNPPQRKKVLSLEYRKRKQEAKEKNSAGGGGSDSAQSKSKSAGAGQGSSNSVSDTGAHGVQSSARTPSSPHKKFSPSHSSASHLEAVSPSD
dr_SETD5	1133	SNPPQRKKVLSLEYRKRKQEAKEKNSAGGGGSDSAQSKSKSAGAGQGSSNSVSDTGAHGVQSSARTPSSPHKKFSPSHSSASHLEAVSPSD
hs_SETD5	1148	SRGTSSSHCRPOENISSRWVPTSVERLREGGS-IPKVLRSVSRVAQKGEPSB-TWESNITEKSDPADGEGPPLSSALSKGATVYSPS
mm_SETD5	1147	SRGTSSSHCRPOENISSRWVPTSVERLREGGS-IPKVLRSVSRVAQKGEPSB-TWESNITEKSDPADGEGPPLSSALSKGATVYSPS
dr_SETD5	1208	VKSG-----NHTKSNHMVPTSVERLREGGAGAEVRLRGNINIERALKRADAGINDLISQPKS-SLVVEMRLSSLA---SPTKSPS
hs_SETD5	1236	RYSY-QLLOCDSPRTEQSLLQOQSSSPFRGHPTQSPGYSYRTTALRPGNPPSHGSSSESLSSTSYSSPAHF-VSTDLSLAPFTGTPGYFSS
mm_SETD5	1235	RYSY-QLLOCDSPRTEQSLLQOQSSSPFRGHPTQSPGYSYRTTALRPGNPPSHGSSSESLSSTSYSSPAHF-VSTDLSLAPFTGTPGYFSS
dr_SETD5	1287	VHPHQQMLPL-K-----ESHQHLESPATDQOQSS-----SSPFCPSVSPSPRPSSEGFAYFSS
hs_SETD5	1324	QPHSGNSTG-----SNLPRRSCPSAASPTLQGPSDSPTSDSVQSSTGTLSSSTFPQNSRSSLPSDLRTISLPSA---GQSA
mm_SETD5	1323	QPHSGNSTG-----SNLPRRSCPSAASPTLQGPSDSPTSDSVQSSTGTLSSSTFPQNSRSSLPSDLRTISLPSA---GQSA
dr_SETD5	1340	KLPVHSPILGSPSSSTVSTSSLDSTVCAPHAHSSSAGAMDSSSLKA--KLLDSSLRAIACMPAR--GHKLD--DASVPTQGAHGR
hs_SETD5	1399	VYQASR----VSAVNSQHYPHRGGSGGVHGYRLQPLQSGVKTOTGLS
mm_SETD5	1398	VYQASR----VSAVNSQHYPHRGGSGGVHGYRLQPLQSGVKTOTGLS
dr_SETD5	1424	LAQTERIQSQRI DRANQANSRLTSPGAQHY PQRNLOGSGVKTOTGLS

Figure 1: Zebrafish *setd5* displays a high amino acid sequence homology to human and murine SETD5 within the SET domain. Amino acid sequence alignment of human (hs) (NCBI: NP_001073986.1), murine (mm) (NCBI: NP_082661.1) and zebrafish (dr) (NCBI: XP_698834.4) Setd5 Isoform 1. Identical amino acids shaded in black, amino acids with similar chemical properties are shaded in grey. The SET domain of each species is highlighted by a red box.

3.2 *Setd5* is ubiquitously expressed in zebrafish from early developmental stages on

The first step in order to investigate *setd5* function *in vivo* was to assess whether *setd5* is already expressed at the first stages of embryonic zebrafish development. Therefore, a semi-qualitative PCR on cDNA of wildtype embryos at different developmental stages was performed and detectable amounts of *setd5*-amplificates were visualized by Gel Electrophoresis (Figure 3, A).

This experiment proved *setd5* expression at all tested embryonic stages of zebrafish development. The presence of *setd5* mRNA indicates a possible gene function during development.

To further elucidate the temporal and spatial expression of *setd5* in zebrafish during embryogenesis, a whole-mount *in situ* hybridization (WISH) evaluated *setd5* transcription on RNA level (Figure 2, B-K).

Setd5 mRNA was traceable in all tissues from the early beginning of embryonic development on. Already at 14 somite stage (Figure 2, B,C), *setd5* expression was ubiquitous. At 24hpf, *setd5* expression in the developing brain was clearly noticeable (Figure 2, D,E), as well as in the entire forming embryo. *Setd5* remained ubiquitously expressed also at the further stage of 48hpf (Figure 2: F-H). The developing pectoral fins and the eye clearly showed *setd5* expression, as well as a weak expression in the forming heart tube. Reaching the 72hpf stage, zebrafish embryos maintained the ubiquitous expression pattern of *setd5* emphasizing the eye and the brain, together with a minor expression in the heart (Figure 2: I-K).

Taken together, the studies showed temporal *setd5* expression throughout all stages of embryonic development and spatial expression ubiquitously in all tissues including a weak expression in the heart.

Results

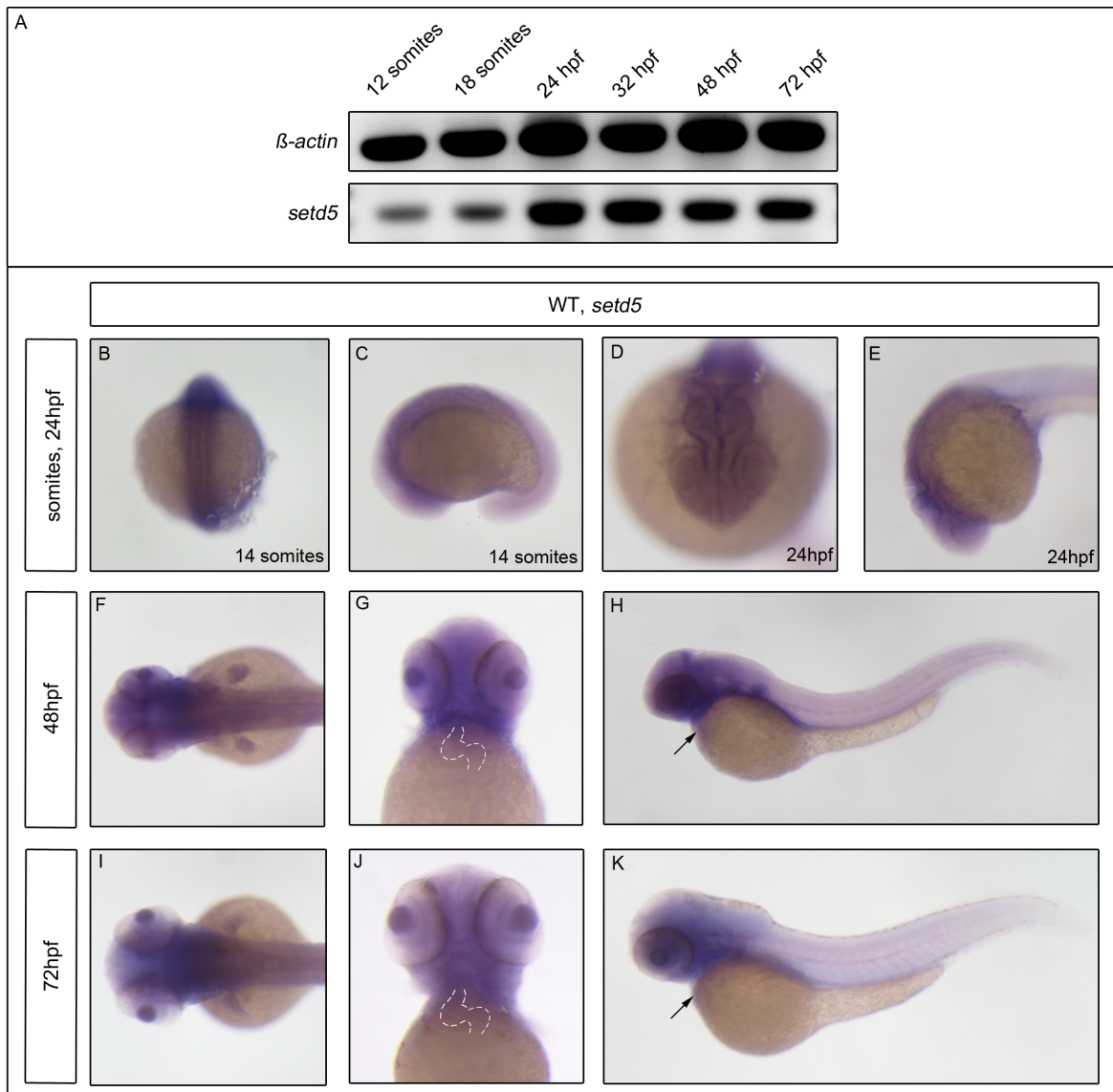


Figure 2: *Setd5* is ubiquitously expressed in all developmental stages. (A) Wildtype cDNA of different developmental stages. *Setd5* amplicates are detectable at all stages of development. Primers against β -actin sequence served as a positive control. **(B-K)** Whole mount *in situ* hybridization demonstrated *setd5*-mRNA expression in wildtype embryos at different embryonic stages: (B,C) 14 somite stage; (D,E) 24hpf; (F-H) 48hpf; (I-K) 72hpf. (B,F,I) dorsal view; (C,E,H,K) lateral view; arrowheads mark the heart position (D,G,J) ventral view; implied heart shapes are shown as dashed lines.

3.3 Localization of Setd5 on cellular level

Since SETD5 shares high sequence homology across vertebrate species and since *setd5* is ubiquitously expressed at all early stages of zebrafish development, it was then interesting to investigate the protein localization within the cell. Specific protein localization to a certain cellular compartment can imply a potential protein function. In cell lines from human kidneys (HEK293T), from hearts of neonatal mice and adult zebrafish, Setd5 localization experiments were performed using Tol2pA2[CMV:setd5:eGFP]-plasmid transfection or antibody staining (Figure 3).

In all cell culture experiments, co-staining with 4',6-diamidino-2-phenylindole (DAPI) was performed. DAPI bound A-T-rich regions of DNA and therefore marked nuclei in blue (Figure 3, A,E,I,M,Q,U). Cell membranes were highlighted in red through co-staining with β -Catenin-antibody, since β -Catenin functions in cell-cell adhesion (Figure 3, C,G,K,O,S,W). Setd5 localization was always presented in green. A digital merge of all three channels was generated to emphasize Setd5 localization in regard to the nucleus and the cell membrane.

For the plasmid transfection, multisite gateway cloning generated a plasmid composed of the pDestTol2pA2 backbone, a 5' CMV promotor sequence, the no-stop variant of *setd5* and a 3' eGFP tag. The delivery of plasmid DNA to the HEK293T cells was accomplished using lipofectamin 2000. Transfection worked successfully if the cells showed green fluorescence. One day after transfection, the human kidney cells presented either a nuclear (Figure 3, A-D) or cytoplasmic (Figure 3, E-H) Setd5 expression.

Primary cultures of neonatal mouse cardiomyocytes were fixed and stained with immunofluorescence antibodies directed against Setd5. Both, the Setd5-N-term-antibody (Figure 3, I-L) and the Setd5-polyclonal-antibody (Figure 3, M-P) showed nuclear and cytoplasmic Setd5 expression in neonatal murine cardiomyocytes.

Adult zebrafish cardiomyocytes were isolated, cultured and fixed prior to staining. Setd5-N-term-antibody detected nuclear and cytoplasmic Setd5 (Figure 3, Q-X), comparable to the murine cells. Nuclear expression appeared to be stronger in comparison to the cytoplasm.

Results

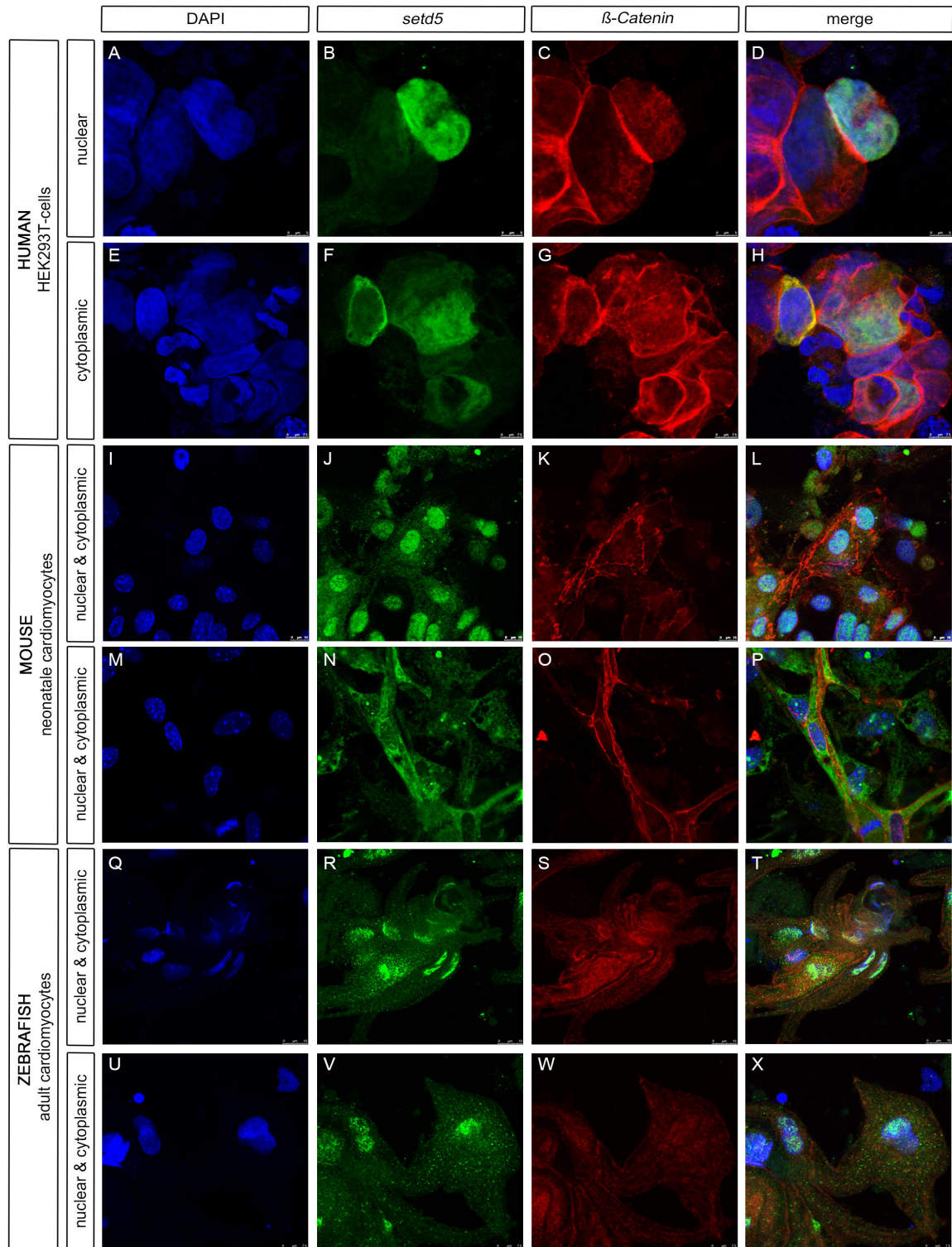


Figure 3: Setd5 localizes in both, cytoplasmic and nuclear cell compartment. (A-H) Transfection of human HEK293T cells with Tol2pA2[CMV:setd5:eGFP] plasmid (green). **(I-P)** Immunofluorescence antibody staining of Setd5 (green) using Setd5-N-term-antibody (I-L) and Setd5-polyclonal-antibody (M-P) on neonatal murine cardiomyocytes. **(Q-X)** Immunofluorescence antibody staining of Setd5 (green) using Setd5-N-term-antibody on adult zebrafish cardiomyocytes. Co-staining with β -Catenin (red) (C,G,K,O,S,W) and 4',6-diamidino-2-phenylindole (DAPI) (blue) (A,E,I,M,Q,U).

Results

All in all, Setd5 was traceable to cytoplasm and nucleus in all three studied cell populations. Cardiomyocytes of mouse and fish showed predominately nuclear expression, together with a minor expression in the cytosol. Human Setd5 expression was restricted to either one of the two compartments.

3.4 Knockdown of *setd5* leads to heart defects during early zebrafish development

In order to investigate the role of *setd5* in vertebrate heart development and its function *in vivo*, a Morpholino-modified antisense oligonucleotide mediated knockdown study was performed in zebrafish embryos. Therefore, Morpholinos (MO) directed against the splice donor site of exon 10 (MO1-*setd5*) and the translational start-site (MO2-*setd5*) were injected into one-cell stage embryos.

MO1-*setd5* efficacy was greater than MO2-*setd5*, therefore MO1-*setd5* was injected at a lower 200µM concentration in comparison to MO2-*setd5*, which was injected at 700µM. For each Morpholino, a five base-pair mismatch Morpholino was designed, injected at the same concentration as the corresponding Morpholino and used as a control (MO1-*ctrl* and MO2-*ctrl*). Injected embryos were examined at 48hpf and 72hpf using light microscopy (Figure 4, A-J).

Wildtype (WT) embryos presented regular development and age-appropriate growth (Figure 4, A,B). Both MO1-*ctrl* (Figure 4, C,D) and MO2-*ctrl* (Figure 4, G,H) injected embryos closely resembled their wildtype siblings at the respective developmental stage.

At 48hpf, MO1-*setd5* injected embryos presented a prominent pericardial edema and a smaller head size compared to the wildtype fish (Figure 4, E). At 72hpf, head and brain were clearly smaller and underdeveloped in comparison to their wildtype siblings. The eyes were remarkably undersized; the entire embryos axis was curved and the pericardial edema increased in volume. The heart was hard to distinguish because of its smaller size and its stretched shape (Figure 4, F).

MO2-*setd5* morphants closely corresponded to the MO1-*setd5* morphants and displayed a smaller head size, brain malformation, a curved body axis and an

Results

even stronger pericardial edema. Again, the heart was thin and stretched, clearly not resembling the heart of wildtype embryos (Figure 4, I,J).

To assure that the observed phenotype is due to a knockdown of *setd5* caused by Morpholino injection, a splice-assay and Western-Blot analysis were performed (Figure 4, K-L). MO1-*setd5* is predicted to alter splicing at the exon10-intron11-

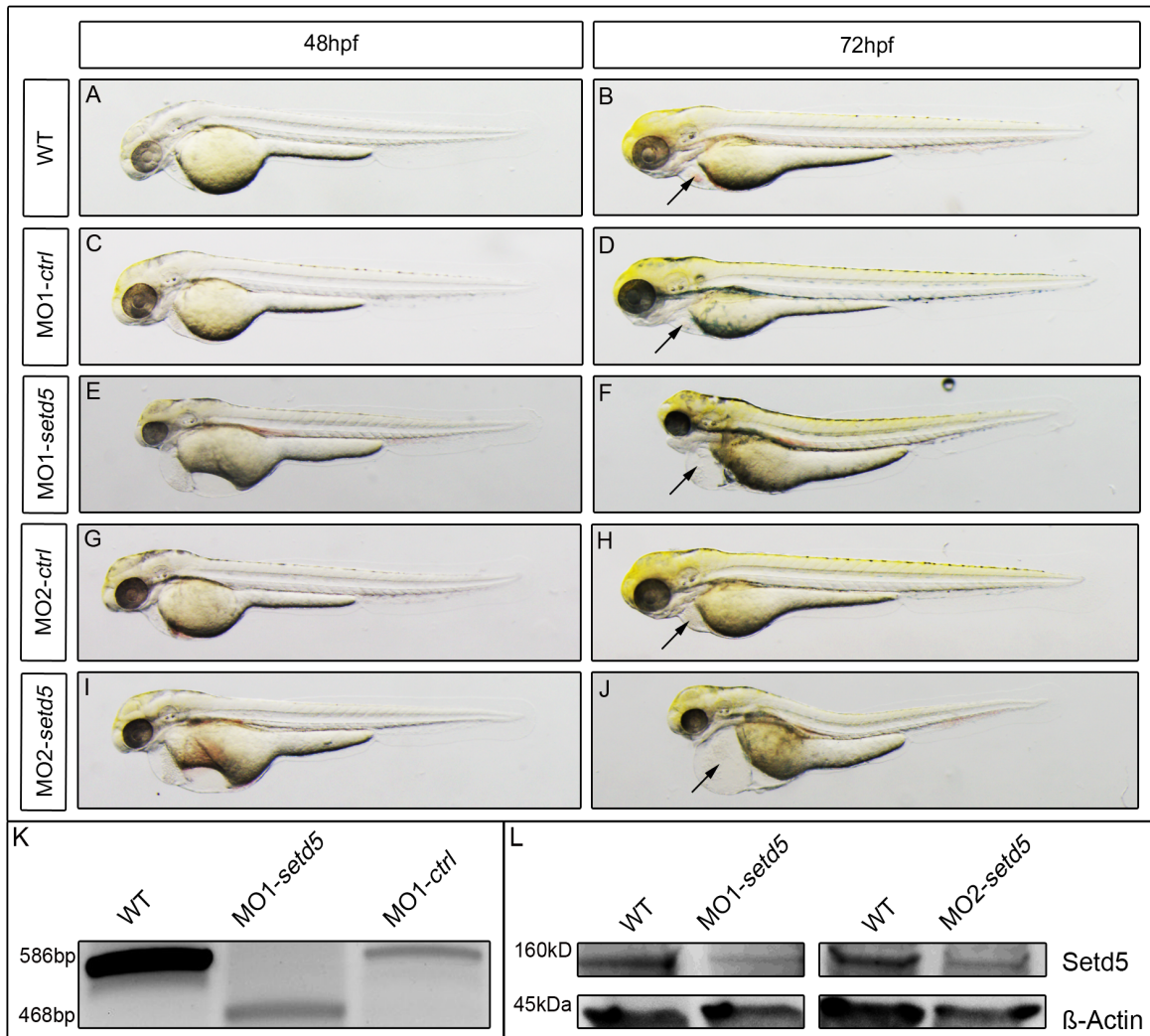


Figure 4: *Setd5* knockdown results in a specific heart phenotype. (A-J) Lateral views of zebrafish embryos at 48hpf (A,C,E,G,I) and 72hpf (B,D,F,H,J). (A,B) Uninjected wild-type embryos (WT). (C,D,G,H) Corresponding five-base-pair-mismatch control Morpholino (MO-ctrl) injected embryos. (E,F,I,J) Morpholino-mediated knockdown of zebrafish *setd5* through injection of 200 μ M MO-*setd5* (E,F) or 700 μ M MO2-*setd5* (I,J). Arrowheads mark the heart position.

Morpholino-control-experiments proof loss of *Setd5* due to knockdown. (K) Splice-assay on cDNA at 48hpf with primers covering the splice-site targeted by MO1-*setd5* (L) Western-Blot analysis of protein lysates of wildtype (WT) and Morpholino injected embryos (MO-*setd5*) at 72hpf.

Results

boundary. Amplification of the zebrafish wildtype sequence between exon 9 and exon 13 resulted in a 586bp cDNA fragment, whereas the fragment of MO1-*setd5* injected embryos was with a length of 468bp shorter. The morphant band's loss of 118bp indicates a skipping of exon 10 as a consequence of Morpholino induced splice alteration (Figure 4, K). The loss of exon 10 on mRNA level due to MO1-*setd5* injection results in a frame shift and subsequently in a stop codon shortly after exon 9.

Western-Blot analyses using Setd5 antibody on protein-lysates of Morpholino injected embryos at 72hpf were performed to assure loss of Setd5 protein (Figure 4, L). Both MO1-*setd5* and MO2-*setd5* injection led to a loss of Setd5 on protein level.

Taken together, both Morpholinos directed against *setd5* resulted in a severe alteration in translation of mRNA and therefore to a loss of function of *setd5*. A sufficient loss of Setd5-protein can be obtained by Morpholino-mediated knockdown, which clearly impairs zebrafish development in multiple organ systems. The most prominent effects of Setd5 knockdown were the pericardial edema and the heart shape alteration, pointing at potential cardiac defects.

3.5 Knockdown of *setd5* leads to cardiac arrhythmia

Since the most prominent observed phenotype was the pericardial edema and the small and stretched heart, further attention was drawn towards the cardiac phenotype. First, heart morphology and function behind the prominent pericardial edema were investigated.

High magnification light microscopy of zebrafish hearts revealed a highly-altered heart morphology in *setd5*-knockdown embryos (Figure 5, A-D). At 72hpf control-injected embryos showed a looped, two chambered heart (Figure 5, A, C). Atria and ventricles were well developed and clearly separated by the atrioventricular canal. MO1-*setd5* and MO2-*setd5* injected embryos at 72hpf presented a smaller heart compared to the control-injected embryos, which was surrounded by a large pericardial edema (Figure 5, B, D). The atrium was stretched and thin, whereas the ventricle appeared to be small and lumpy.

Results

Focusing on the heartbeat, control-injected fish displayed a rhythmically beating atrium and a ventricle similar to their wildtype siblings. Injection of Morpholinos targeting *setd5* led to an arrhythmic heartbeat. MO-*setd5* injected embryos presented a totally silent ventricle where no ventricular contraction was detectable (Figure 5, E-F). The atrial cardiac activity displayed diverse forms of arrhythmia in different MO-*setd5* injected embryos. Some atria were contracting regularly, whereas atria of other embryos showed atrial fibrillation or complete atrial arrest. Quantification proved that this phenotype of atrial arrhythmia and ventricular arrest is specific for both Morpholinos targeting *setd5* (Figure 5, E-F). 94.82% \pm 1.29 of MO1-*setd5* or 91.70% \pm 0.94 of the MO2-*setd5* injected embryos displayed this distinct cardiac phenotype whereas MO-*ctrl* injected embryos were devoid of any

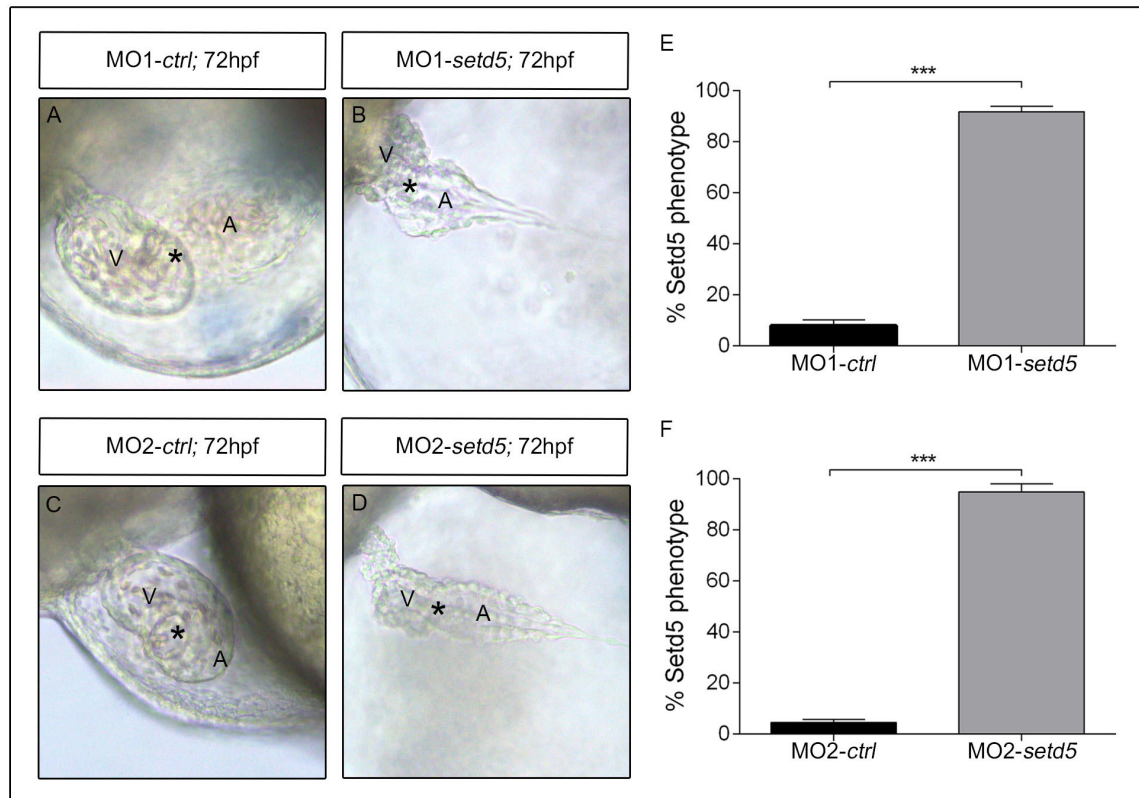


Figure 5: Loss of *setd5* causes atrial arrhythmia and ventricular arrest. (A-D) *In vivo* hearts of control-injected (A,C) and Morpholino-injected (B,D) embryos at 72hpf. A marks the atrium and V the ventricle. Asterisks mark the atrioventricular canal. The phenotype was defined by atrial arrhythmia and ventricular arrest. **(E,F)** According to this definition, n=1107 injected embryos (E) and n=816 injected embryos (F) at 48hpf were scrutinized and counted for percentage phenotype in 5 independent experiments. More than 94.82% \pm 1.29 of MO1-*setd5* or 91.70% \pm 0.94 MO2-*setd5* injected embryos display lack of cardiac contractility. Asterisks indicate a significant difference of $p \leq 0.0001$.

Results

abnormalities (MO1-ctrl 4.46% \pm 0.51; MO2-ctrl 7.88% \pm 1.05).

Knockdown of *setd5* causes severe heart morphology defects, combined with cardiac arrhythmia and a lack of ventricular contraction in zebrafish.

3.6 Loss of *setd5* results in heart morphology changes

To further describe the heart morphology defects seen by light microscopy, explanted hearts of injected embryos were analyzed using high resolution microscopy. By dissecting hearts of MO1-*setd5* and control injected embryos at 72hpf, fixation and immunofluorescence staining, a close look was taken at the explanted hearts (Figure 6). Cardiomyocytes were marked by myocyte-specific enhancer factor 2 (MEF2) and nuclei were counterstained with DAPI.

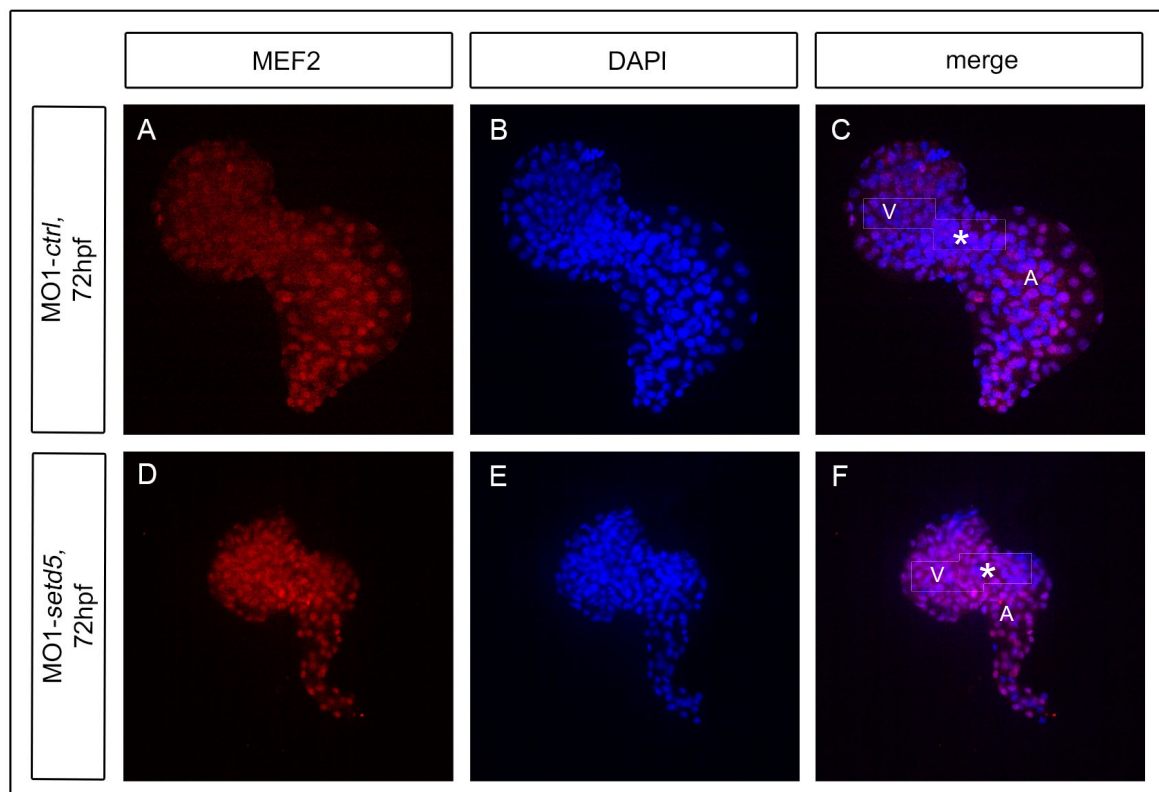


Figure 6: Loss of *setd5* causes a characteristic heart morphology. Immunostaining of dissected hearts of MO1-ctrl (A-C) and MO1-*setd5* (D-F) injected embryos at 72hpf. A marks the atrium, V the ventricle, asterisks indicate the atrioventricular canal (AVC). Staining with myocyte-specific enhancer factor 2 (MEF2) indicates cardiomyocytes (A,D). 4',6-diamidino-2-phenylindole (DAPI) marks nuclei (B,E).

Results

Hearts of MO1-*ctrl* injected embryos presented a uniform distribution of cardiomyocytes throughout the atrium and the ventricle, which were clearly detectable and divided by the atrioventricular canal (AVC) (Figure 6, A-C). In hearts of MO1-*setd5* injected embryos (Figure 6, D-F), cardiomyocytes appeared to be less in number in the atrium compared to control-injected embryos. The MO-injected-ventricle seemed to be misshapen and lumpy. In general, both cardiac chambers of MO-injected embryos, atrium and ventricle were smaller in size.

To dissect a potential cause for the dysfunction of the morphants' hearts, the heart morphology was examined further by means of hematoxylin-eosin staining of histological sections of injected embryos (Figure 7, A, D). At 72hpf, in control-injected embryos both chambers were clearly distinguishable, divided by the atrioventricular canal (AVC). Endocardium and myocardium appeared as two distinct cell layers. Embryos lacking *setd5* showed considerable differences in

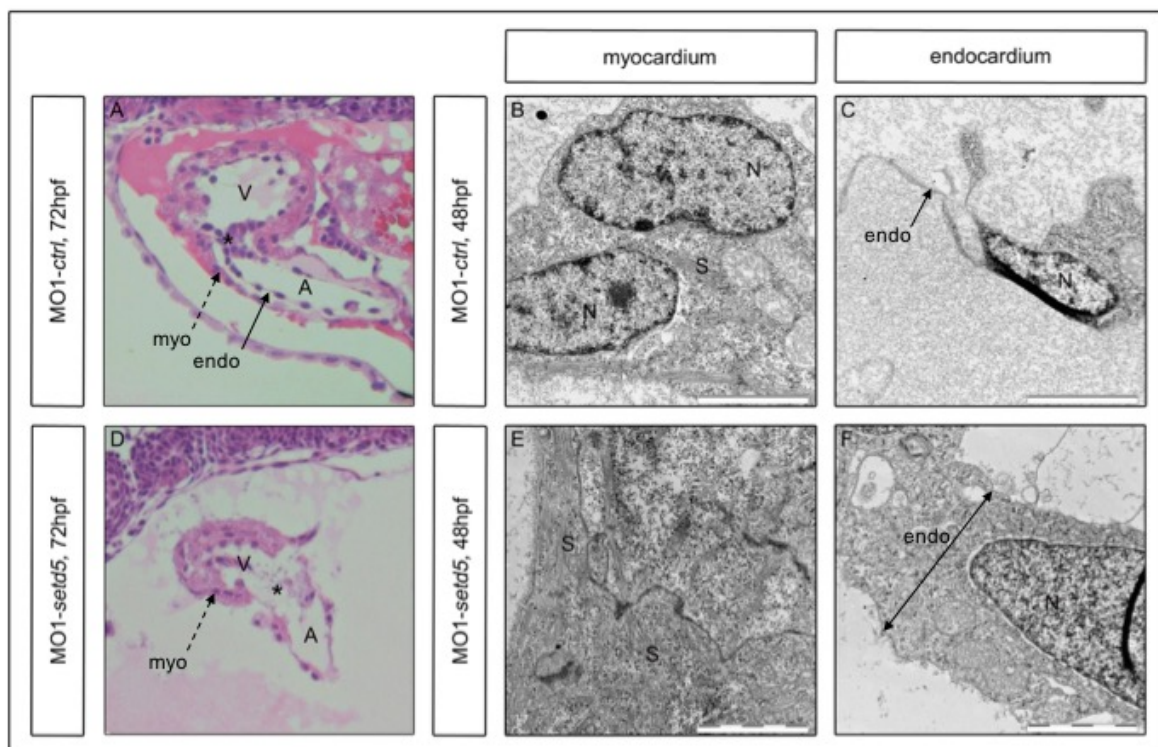


Figure 7: Loss of *setd5* impaires heart morphology. (A,D) Hematoxylin-Eosin staining of histological sagittal crosssections of control (A) and *setd5*-morphant (D) embryos at 72hpf. A=atrium, V=ventricle, endo=endocardium, myo=myocardium, asterisks mark the atrioventricular canal. (B,C,E,F) Electron transmission microscopy of ventricles of MO1-*ctrl* (B,C) or MO1-*setd5* (E,F) injected embryos at 48hpf. Either the myocardium (B,E) or the endocardium (C,F) was in focus. N=nucleus, S=sarcomers.

Results

morphology. The morphant heart presented a broad AVC, a small atrium and a compact ventricle (Figure 7, D). Differentiation between endocardium and myocardium in the *setd5* morphant embryo heart was not as clear as in the wildtype heart.

Therefore ultrastructural analyses via electron transmission microscopy of injected embryos at 48hpf were performed, to provide more detailed information of the heart morphology, especially of the endocardium and the myocardium (Figure 7, B,C,E,F). Injection of MO1-*setd5* in zebrafish embryos resulted in a similar myocardial tissue structure as in control embryos (Figure 7, B,E). The myocardial specific sarcomeric bundles were detectable in both control and knockdown sections. Focusing on the endocardium, severe differences between MO-*ctrl* and MO-*setd5* injected embryos are evident. The control endocardium is thin and mono-layered as known from wildtype fish (Figure 7, C). To the contrary, the endocardial layer of morphant embryos is detached from the myocardium, forming a lump in the middle of the ventricular chamber (Figure 7, F). No sarcomeres were traceable to underline the endothelial origin of this structure.

Morphological examination of *setd5* knockdown embryos showed severe alterations of heart shape and structure due to loss of *setd5*. The endocardial layer seemed to be strongly affected by *Setd5* knockdown.

3.7 *Setd5* is not responsible for endocardial development

Setd5 appeared to be involved in endocardial development, therefore microinjections of MO1-*ctrl* and MO1-*setd5* in embryos of the transgenic line *Tg(fli:eGFP)* were performed (Figure 8). The *fli*-promotor is the earliest known endothelial cell marker driving expression of enhanced green fluorescent protein (eGFP) in this transgenic line to visualize vasculogenesis and endocardial development.

At 48hpf, control injected embryos displayed a uniform patterning of *fli*-positive cells throughout the vascular system (Figure 8, A-C). Close-ups of the tail showed green fluorescence, standing for regular endothelial development. Also in the heart, green fluorescence proved the presence of endocardium. Injection of MO1-*setd5* in *Tg(fli:eGFP)* led to no significant difference in endothelial development

Results

compared to the control (Figure 8, D-F). The presence of endothelium was proved throughout the entire morphant embryo, although not all blood vessels were completely matured. Green fluorescence in the hearts of MO-*setd5* injected *Tg(fli:eGFP)* embryos clearly demonstrated the developed endocardium.

Morphants presented the same fluorescence pattern than control embryos, indicating that *setd5* knockdown does not impair endothelial nor endocardial development.

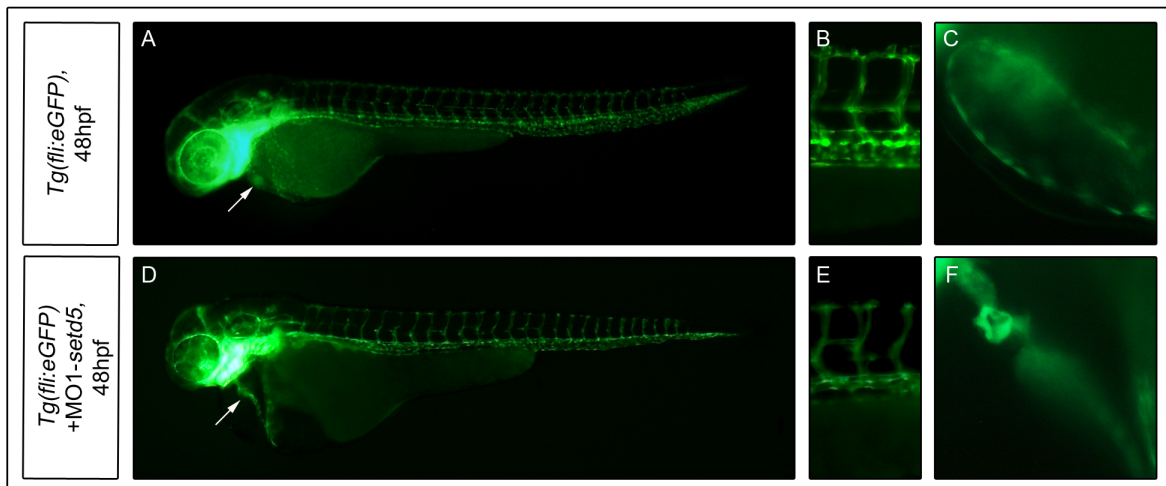


Figure 8: *Setd5*-knockdown does not influence endothelial development. (A-F) Fluorescence imaging after microinjection of MO1-*ctrl* (A-C) and MO1-*setd5* (D-F) in the transgenic zebrafish line *Tg(fli:eGFP)*. Expression of enhanced green fluorescent Protein (eGFP) marks endothelial cells. (A,D) Lateral views of zebrafish embryos at 48hpf. Arrowheads mark the heart position. (B,E) Image detail of the tail. (C,F) Heart-imaging at higher magnification visualizing the endocardium.

3.8 Knockdown of *setd5* shows normal cardiomyocyte differentiation and specification

To assess whether *setd5* knockdown leads to disorders in early embryonic heart development, a whole-mount *in situ* hybridization was performed. Emphasis was put on the most important markers of cardiomyocyte-differentiation: atrial myosin heavy chain (*amhc*), ventricular myosin heavy chain (*vmhc*) and cardiac myosin light chain 2 (*cmlc2*) (Figure 9).

Results

Amhc clearly marked the atrium of control injected embryos and morphants at 48hpf, even the characteristic stretched and small atrium shape of morphant hearts were displayed (Figure 9, A,D). The *vmhc* probe stained the ventricle of control and morphant hearts, again depicting the small and lumpy ventricle after MO1-*setd5* injection (Figure 9, B,E). The entire heart outline was highlighted by the *cmhc2* probe in both control and morphant embryos (Figure 9, C,F). Taken together, cardiomyocyte differentiation is unaffected by *setd5* knockdown.

To determine chamber specification, an S46/MF20 Immunostaining was utilized. The antibodies S46, directed against atrial specific myosin heavy chain, and MF20, directed against sarcomeric myosin heavy chain, highlighted cardiomyocyte specification (Figure 10).

S46 expression was only noticeable in the atria of MO1-*ctrl* and MO1-*setd5*

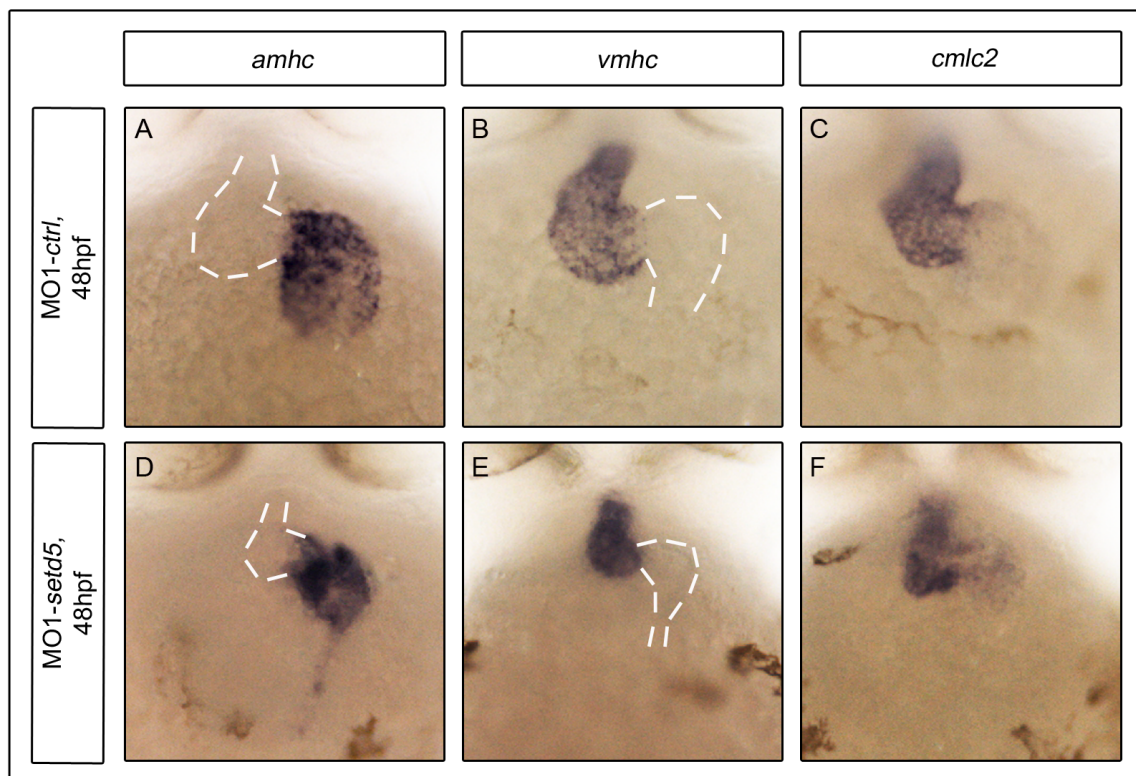


Figure 9: Cardiomyocyte differentiation is unaffected by *setd5* knockdown. Whole mount *in situ* hybridization of MO1-*ctrl* (A-C) and MO1-*setd5* (D-F) injected embryos at 48hpf. Probes were directed against the atrium-specific atrial myosin heavy chain (*amhc*) (A,D), the ventricle-specific ventricular myosin heavy chain (*vmhc*) (B,E) and whole heart specific cardiac myosin light chain 2 (*cmhc2*) (C,F). Implied heart shapes are shown as dashed lines.

Results

injected embryos at 48hpf (Figure 10, A, D). The distinct morphant heart morphology was recognizable in the atrium as well as in the ventricle stained with MF20. Whereas the control heart presented a wide ventricle, the morphant ventricle appeared compressed (Figure 10, B, E). By merging both channels, the atrioventricular canal (AVC) region got highlighted in yellow and was present in control and morphant embryos (Figure 10, C, F).

In both experiments, expression patterns were in a typical heart specific manner, clearly demonstrating that a loss of *setd5* has no influence on cell fate differentiation and specification of cardiomyocytes.

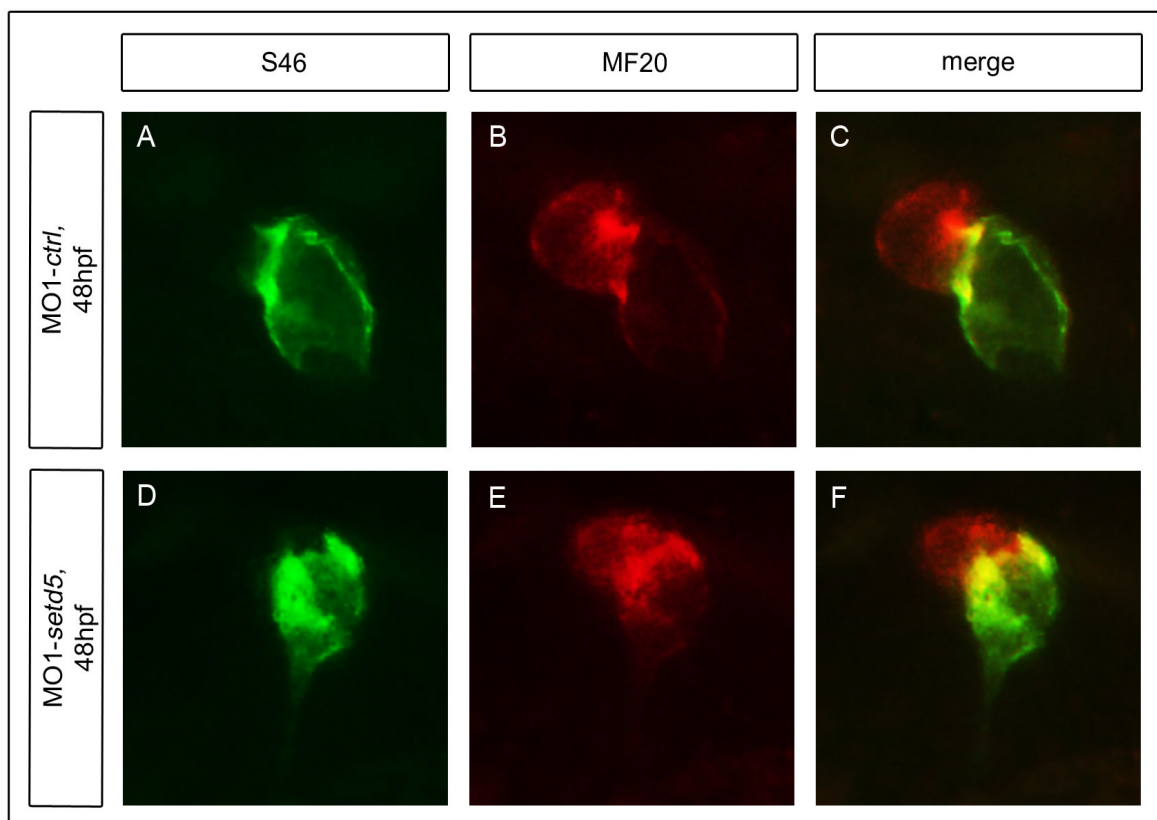


Figure 10: Cardiomyocyte specification is unaffected in *setd5*-morphant embryos. Immunofluorescence staining of whole MO1-*ctrl* (A-C) and MO1-*setd5* (D-F) injected embryos at 48hpf. Atrium specific S46-antibody directed against atrial myosin heavy chain is colored in green (A,D). MF20 marks sarcomeric myosin heavy chains of both chambers which were visualized in red (B,E).

3.9 *Setd5* is essential to maintain cardiac contractile function in zebrafish

3.9.1 *Setd5* knockdown impairs cardiac contractility

To further quantify the cardiac contractile dysfunction of *setd5*-morphants' hearts, atrial and ventricular heart rates were measured at 48hpf and 72hpf (Figure 11). Embryos were adjusted to room temperature and heart beats of atrium and ventricle were counted. In *control*-injected embryos, every atrial heart beat was followed by ventricular contraction, therefore both chambers shared the same heart rate at any time (Figure 11, A,C). The average heart rate at 48hpf of 126.8 ± 12.34 bpm even increased at 72hpf to 141.7 ± 13.32 bpm in MO1-*control* embryos (MO2-*ctrl*: 132.7 ± 12.53 bpm at 48hpf, 151.9 ± 7.28 bpm at 72hpf). *Setd5*-morphants had no noticeable ventricular heartbeat at any point of observation (MO1-*setd5* and MO2-*setd5*: 0 bpm at 48hpf and at 72hpf) (Figure 11, B,D). Morphants' atrial chambers were able to contract; however the atrial heart

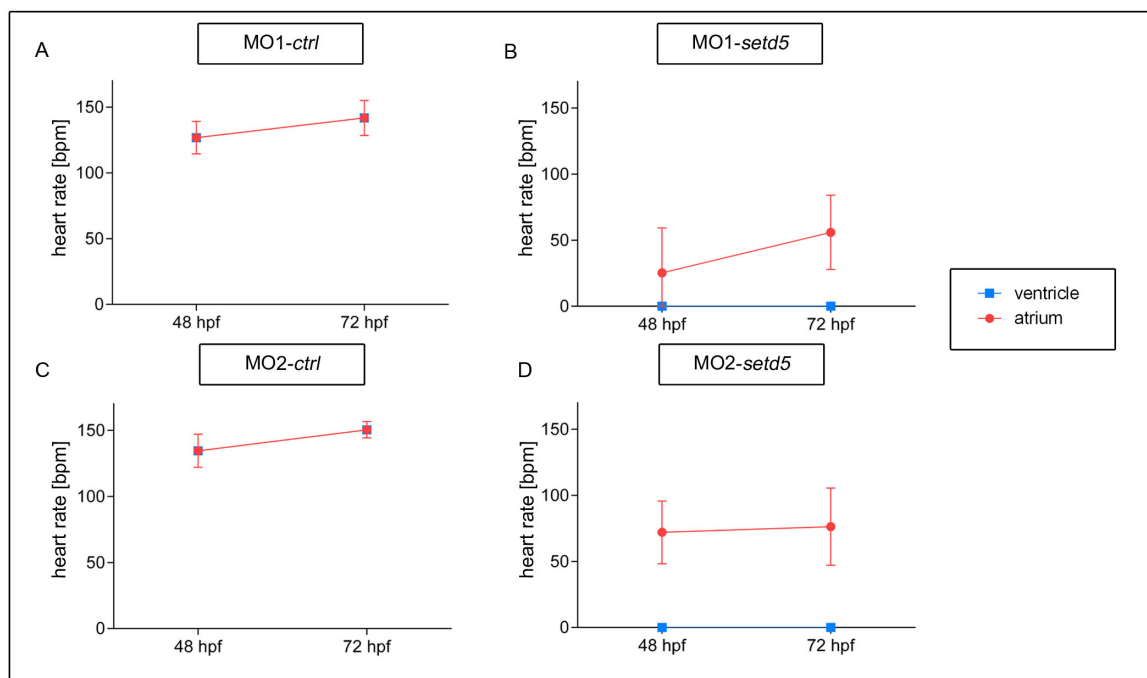


Figure 11: Loss of ventricular heart beat due to *setd5* knockdown. (A-D) Heart beat light microscopy analysis of MO-*ctrl* (A,C) and MO-*setd5* (B,D) injected embryos at 48hpf and 72hpf. The heart rate was manually counted for the atrium (red) and the ventricle (blue) in three individual experiments. n=175

Results

rate was perceptible lower compared to their *control*-injected siblings. Phases of atrial fibrillation were not counted as an atrial contraction. Especially the atrial heart rate of MO1-*setd5* injected embryos increased from 16.56 ± 29.40 bpm at 48hpf to 54.31 ± 35.99 bpm at 72hpf. Atria of MO2-*setd5* injected embryos beat more constantly at rates of 73.59 ± 22.92 bpm at 48hpf and 84.63 ± 29.74 bpm at 72hpf, but still about half as slowly as control-injected embryos.

Next, to evaluate the cardiac contractile force, measurements of chamber specific fractional shortening were undertaken (Figure 12). Videos of embryos at 48hpf and 72hpf were used to acquire chamber diameters at the end of contraction (systole) and the end of relaxation (diastole). Fraction shortening was calculated with the help of the fractional shortening formula, putting systolic and diastolic chamber diameters in relation (see 2.2.5). With the help of the fractional shortening rate conclusions can be drawn regarding cardiac contractility.

Fractional shortening of the atrium differed slightly between MO-*ctrl* and MO-

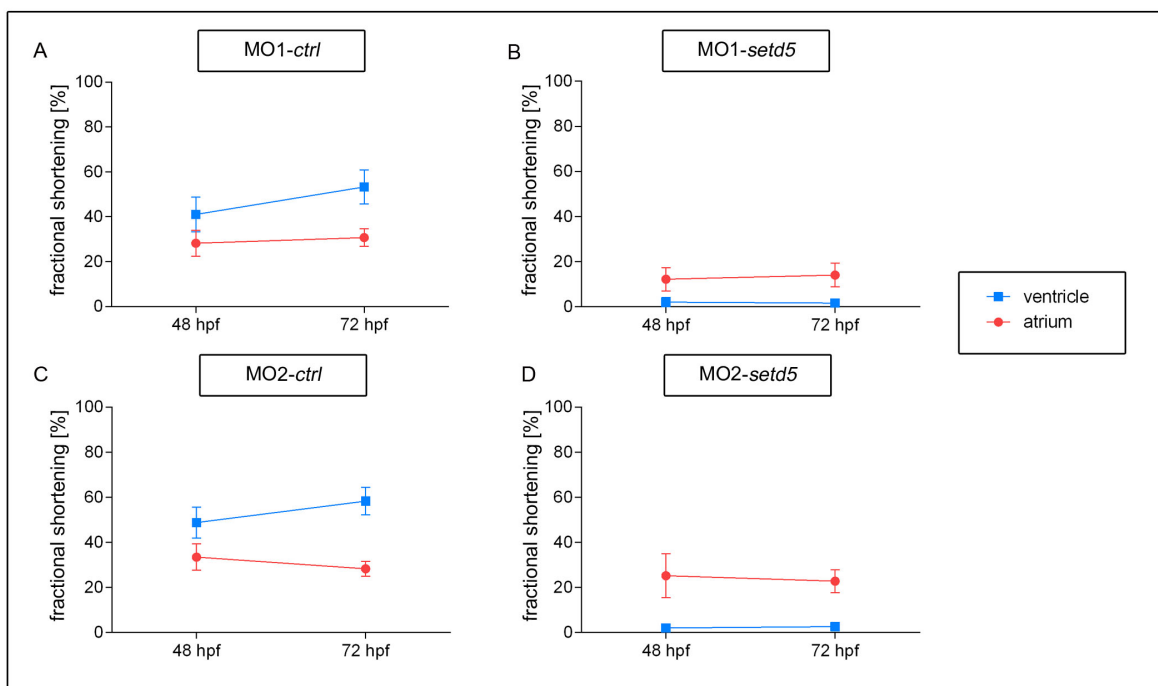


Figure 12: Setd5 knockdown impairs ventricular contractility. Videos of MO-*ctrl* (A,C) and MO-*setd5* (B,D) at 48hpf and 72hpf were used to quantify the atrial (red) and the ventricular (blue) fractional shortening in three individual experiments. n=177

Results

setd5. Atria of MO1-*ctrl* injected embryos displayed a fractional shortening of 28.20 ± 5.75 % at 48hpf and of 30.33 ± 3.41 % at 72hpf (MO2-*ctrl*: 33.44 ± 5.81 % at 48hpf and 28.30 ± 3.22 % at 72hpf) (Figure 12, A,C, red). With a fractional shortening of 12.20 ± 5.13 % at 48hpf and 14.07 ± 5.31 % at 72hpf, the atria of MO1-*setd5* injected embryos presented a slightly smaller cardiac contractile force (MO2-*setd5*: 22.24 ± 5.90 % at 48hf and 22.75 ± 5.00 % at 72hpf) (Figure 12, B,D, red).

Quite contrary to the atrium, the ventricular chamber of morphant-hearts hardly presented a measurable difference in diameter between systole and diastole. Ventricles of MO1-*ctrl* injected embryos displayed fractional shortening of 41.00 ± 7.72 % at 48hpf and increased the contractile function to 53.04 ± 7.62 % at 72hpf (MO2-*ctrl*: 48.78 ± 6.83 % at 48hpf and 58.33 ± 6.01 % at 72hpf) (Figure 12, A,C, blue). MO1-*setd5* ventricles had almost no ventricular contractile force at all with fractional shortening rates of 1.73 ± 1.52 % at 48hpf and 1.66 ± 0.92 % at 72hpf (MO2-*setd5*: 1.76 ± 1.43 % at 48hpf and 2.65 ± 1.04 % at 72hpf) (Figure 12, B,D, blue).

Taken together, heart beat analyses of *setd5* morphant embryos presented atrial arrhythmia and bradycardia, whereas the ventricle remained silent at all times. Fractional shortening measurements clearly showed that *setd5* knockdown restrained cardiac contractility, especially in the ventricle.

3.9.2 *Setd5* is necessary for proper cardiac excitation generation

Potential causes for arrhythmia development lie within the cellular processes between cardiomyocyte excitation initiation, excitation propagation and excitation-contraction coupling. At the myoneural junction, a small influx of calcium into the cell, via voltage-dependent L-type calcium channels, triggers the release of vast amounts of calcium from the sarcoplasmic reticulum, the so called calcium-induced-calcium-release. The high intracellular calcium level initiates myofilamental contraction by calcium binding to Troponin C.

The fluorescent dye Calcium-Green-1 dextran uncovers an increase of intracellular calcium concentration by enhanced fluorescence intensity. Since simple heart contraction increases muscle tissue density, also leading to an increase in fluorescence, it was important to only capture changes in fluorescence caused by

Results

electrical excitation. The zebrafish mutant *flatline* was introduced to conquer this problem. *Flatline* embryos show normal heart development but no heartbeat due to a *smyd1b* mutation. *Smyd1b* is needed for proper skeletal and cardiac muscle function.

In order to investigate the key players of arrhythmogenesis in *setd5*-morphants, calcium transients of MO1-*ctrl*/*setd5* and Calcium-Green1 dextran injected *flatline* embryos were measured at 72hpf. High-speed fluorescence videos were recorded

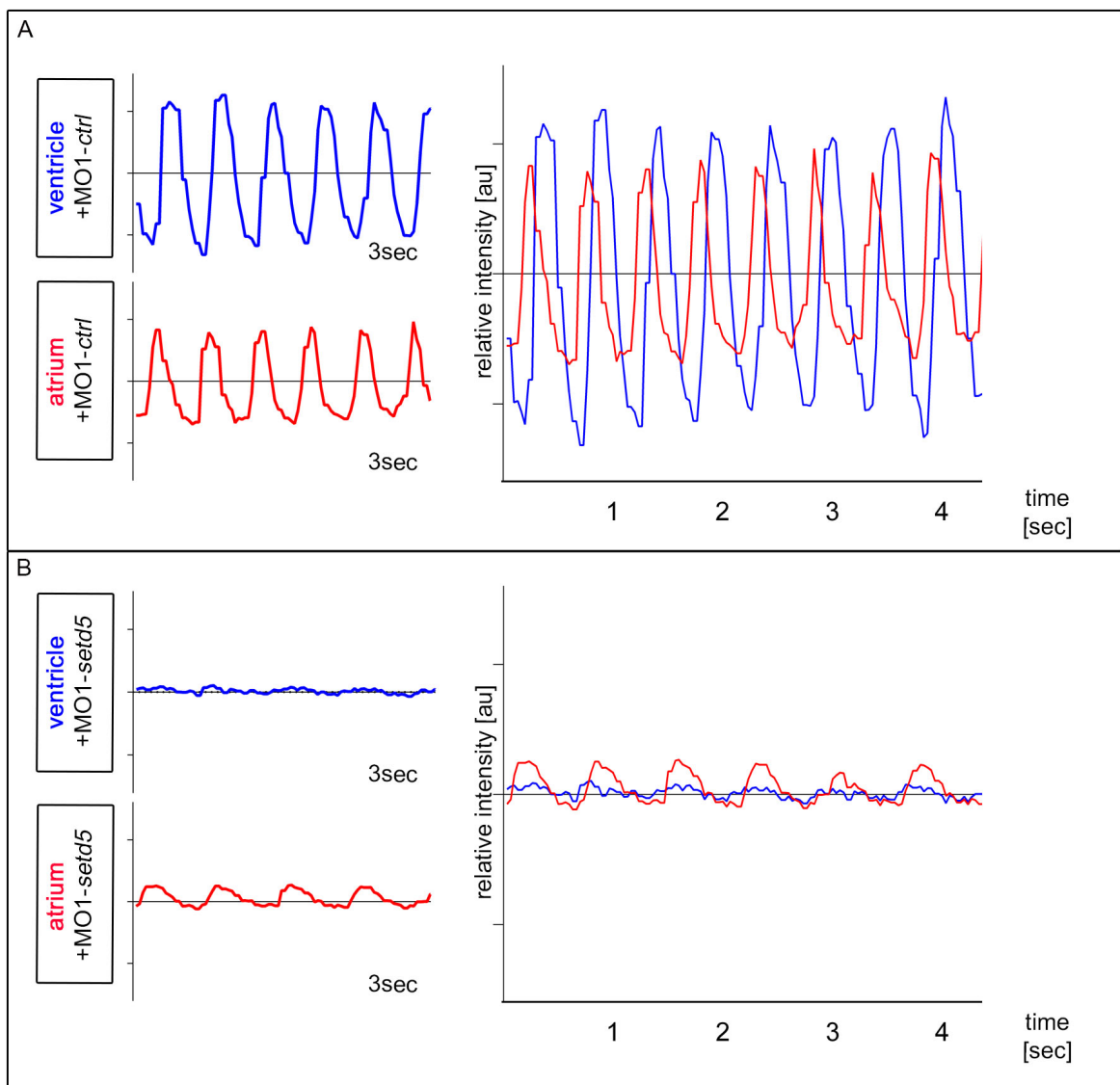


Figure 13: Calcium-imaging of *setd5*-morphants reveals dysfunctional excitation in zebrafish hearts. Recordings of atrial (red) and ventricular (blue) cytosolic calcium transients at 72hpf after MO1-*ctrl* (A) or MO1-*setd5* (B) and calcium green-1 dextran co-injection in *flatline* mutant embryos. The left side displays cardiomyocyte excitation of atrium and ventricle separately whereas the right side demonstrates the excitation time curve of both chambers in relation to each other.

Results

and analyzed. In a movie of an injected *flatline* embryo, a small square in either the atrium or the ventricle was selected, in which changes of fluorescence were graphed over time (Figure 13). Thereby, spatio-temporal conduction was graphed since electrical excitation starts in the atrium and reaches the ventricle with a small AVC caused conduction delay.

In *control*-injected embryos, the calcium wave started at the sinus venosus and propagated fluently throughout atrium and ventricle. Ventricular impulses followed the atrial excitation constantly and with the expected brief delay caused by the AVC. *Setd5*-morphants had no clear, coordinated excitation wave running over their hearts. Ventricular cardiomyocytes did not depict more than subtle changes of intercellular calcium levels, indicating insufficient electrical excitation. Focusing on the atrium, cardiomyocytes were capable of coordinated impulse propagation, implying a normal excitation generation. Even though the fluorescence intensity was lower, atrial action potentials were rhythmic and regular, but slower compared to the control, underlining the previously described bradycardia. The coordinated electrical atrial activity could not propagate in the ventricle. Also, no ventricular escape rhythm was evident.

Setd5-knockout seems to have effected early stages of electrical excitation of ventricular cardiomyocytes. The atrial conduction tissue of *setd5* morphants was capable of regular excitation propagation.

3.10 *Setd5* is involved in histone methylation and acetylation

To discover a potential molecular function of *Setd5* as chromatin modifier, Western Blot analyses were performed using antibodies directed against either methylated or acetylated histones (Figure 14).

In order to explore the predicted methyltransferase activity, protein levels of Methylated Lysine were compared in protein lysates of wildtype or MO1-*setd5* injected embryos. The applied antibody against Methylated Lysine recognized all proteins with methylated lysine residues and did not cross-react with acetylated proteins. No clear difference of lysine methylation was detectable on the protein

Results

level (Figure 14, A, left panel). Thereby, the resolution of this Western Blot against methylated lysines did not allow a specific statement about the methylation status of histones (~15kDa). Therefore, the pan-methylated histone H3 antibody was used to specify histone H3 methylation (Figure 14, A, right panel). Knockdown of *setd5* seems to elevate the amount of methylated histone H3.

To further address the chromatin modifying function of *setd5*, protein levels of Acetylated Histone 4 were compared in wildtype and in Morpholino injected embryos at 72hpf. The used antibody was directed against the acetylated lysine residues 5,8,12 and 16 of histone 4. Knockdown of *setd5* through both Morpholinos led to a remarkable loss of histone 4 protein acetylation in MO-*setd5* injected embryos (Figure 14, B).

To deduce from these findings, Western Blotting showed that the loss of Setd5 increased the amount of histone methylation and substantially decreased histone acetylation.

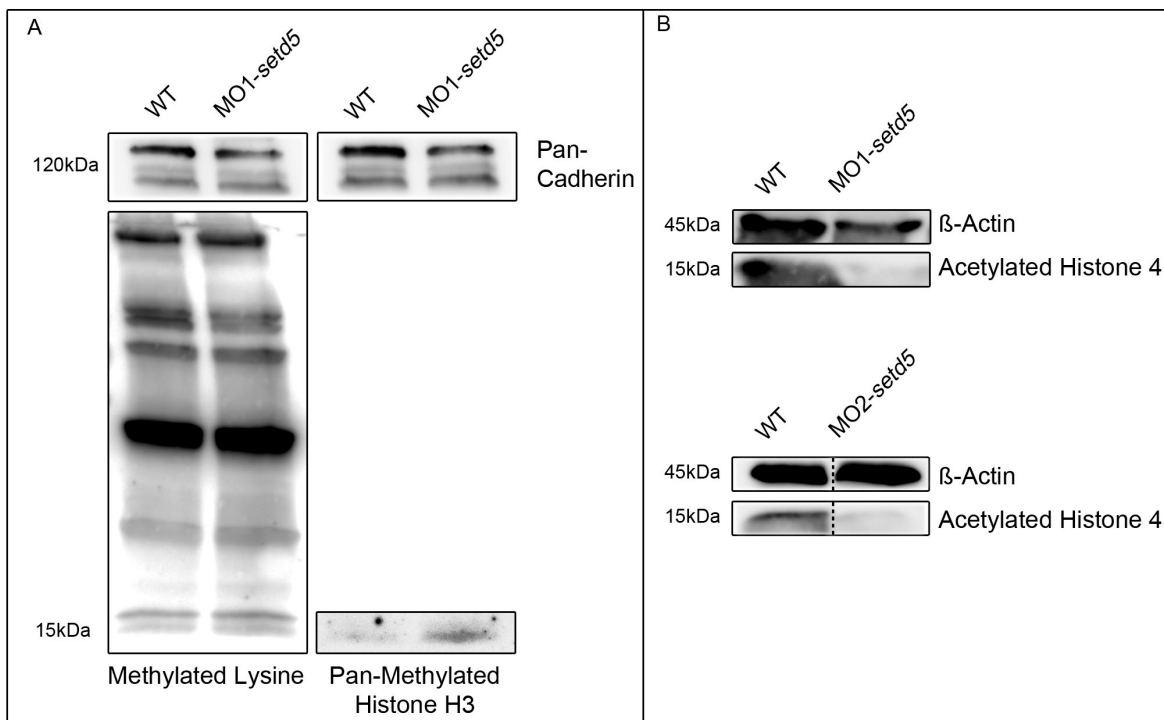


Figure 14: Setd5 takes part in histone methylation and acetylation. Western Blot analysis of Protein lysates obtained from wildtype embryos and *setd5*-morphant embryos at 72hpf. Antibodies were directed against Methylated Lysine, Pan-Methylated Histone H3 (A) and Acetylated Histone 4 (B).

4 Discussion

4.1 *Setd5* shows cross-species homology

The SET domain-containing protein family is evolutionary highly conserved between zebrafish and humans [55]. Amino acid alignment of *Setd5* revealed that the SET domain shows high similarity between human, mouse and fish (see 3.1). Thus, the zebrafish is a suitable model organism to investigate the function of *Setd5 in vivo*. Other known SET domain-containing proteins lack this high degree of interspecies similarity [55].

Immunofluorescent staining showed *Setd5* localization in different cellular compartments. *Setd5* localized to both nuclear and cytoplasmic compartments in cardiomyocytes of mouse and fish (see 3.3). Osipovich *et al.* performed immunofluorescent staining in different murine cells, which revealed a predominantly nuclear expression of SETD5 [39]. The different localization pattern might be caused by the usage of different cells or their observation at different stages of cell development. This makes it difficult to predict a certain cellular function without further detailed investigations.

Closer examination of the whole zebrafish embryo via whole-mount *in situ* hybridization targeting *setd5* on mRNA level showed ubiquitous *setd5* expression throughout all stages of embryonic development with predominant expression in the brain, eye and forming heart tube (see 3.2). These findings are consistent with previous findings of ubiquitous *setd5* expression in *danio rerio* at 24hpf [55] and in embryonic mice at E9.5 [39]. Kuechler *et al.* demonstrated high *setd5* expression in cerebral cortex, intestine and in the eye through semi-quantitative PCR in adult mouse tissue. Low expression was described in kidney, skeletal muscle and spleen [23]. In humans, ubiquitous *setd5* expression was shown, with a prominent higher expression level in the brain [13].

In summary, *Setd5* is ubiquitously expressed in different species throughout different stages of development. Nevertheless, *Setd5* seems to be spatially upregulated in the brain [13, 23]. Interestingly, mutations of *SETD5* in humans lead to intellectual disability [13, 20, 23, 41, 42, 44, 56].

4.2 Loss of *Setd5* leads to defects in cardiac morphology and function

Phenotypical investigations of Morpholino-mediated *Setd5* knockdown in zebrafish were undertaken in order to further assess protein function. *Danio rerio* was chosen as model organism because of the ease of genetic manipulation, the fast, transparent, ex utero development and the ability to survive without a functional circulatory system [2, 7, 36, 46, 54]. Knockdown of *setd5* in zebrafish showed a clear and reproducible phenotype (see 3.4).

The loss of *Setd5* led to a smaller head size and a massive pericardial edema. The abnormal head shape, although not further investigated, is in line with findings in humans, where loss-of-function mutations of *SETD5* cause intellectual disability (ID) [13, 20, 23, 41, 42, 44, 56]. Hence, *SETD5* plays an important role during the development of the brain. Together with certain facial dysmorphisms, *SETD5* mutations in humans contribute to the 3p25 microdeletion syndrome, in whose critical chromosomal region *SETD5* is located [13, 23, 56]. In addition to intellectual disability, patients with a reported loss of *SETD5* are in many cases also affected by congenital heart defects, mostly ventricular and atrial septal defects [13, 23].

Focusing on the heart, detailed investigation on *setd5* knockdown zebrafish embryos displayed an arrhythmic heartbeat, mainly a silent ventricle and an either fibrillating or irregular contracting atrium (see 3.5). In accordance to this, experiments in *Setd5* knockout mice at embryonic age E9.5 led to a similar cardiac phenotype. 50% of the mouse embryos did not show any heart contractions. Pericardial effusions and a disrupted blood flow suggested severe defects in cardiovascular development, due to which the embryos died at E10.5 [39].

Further experiments were undertaken in order to search for morphological defects of the heart caused by *Setd5* knockdown (see 3.6). By histological analysis of zebrafish embryos after *Setd5* knockdown, a single-layered atrium, a broad AVC and a single cell layer of either myocardial or endocardial origin was found. This is in agreement with findings in the *setd5* knockout mouse model of Osipovich *et al.*. Knockout mice at E9.5 displayed an unlooped and underdeveloped heart, with a thin myocardium and reduced ventricular trabeculation [39].

Discussion

Electron microscopy studies of zebrafish hearts at 48hpf could not depict morphologic differences in myocardial architecture. Further studies should investigate the process of ventricular myocardial trabeculation in *setd5* morphants at later stages of development, since alterations in ventricular morphology could explain the dysfunctional ventricle.

Focusing on the heart function of *setd5* morphant embryos, a distinct phenotype could be described by heart rate and fractional shortening analyses, as well as with calcium imaging. Loss of *setd5* in the heart led to atrial bradycardia and atrial fibrillation, together with a complete ventricular arrest. Heart physiology is highly complex, from excitation generation in pacemaker cells, through cardiac conduction via the atrium, AVC and ventricle to electromechanical coupling [18, 43].

The observed atrial bradycardia can be caused by defects in impulse formation through pacemaker cells [18]. The proper formation of the pacemaker in *setd5* morphant embryos should be analyzed with the help of the transcription factors T-box transcription factor 3 (Tbx3) or LIM domain transcription factor Islet-1 (Isl1) [57]. Atrial fibrillation is caused by rapid focal ectopic firing or excitation reentry [17]. None of these phenotypes were confirmed via calcium imaging, which presented a regular and rhythmic atrial excitation wave (see 3.9.2). Although electrical excitation was detectable in the atrium, the ventricular cardiomyocytes presented no coordinated action potential waves. This could have been caused by either defects in excitation propagation via the atrioventricular canal (AVC) and throughout the ventricle, or by defects in electromechanical coupling [18]. Malfunction in excitation conduction within the AVC is supported by the zebrafish mutant line *island beat*. This mutant lacks an alpha1C subunit of L-Type calcium channel (LTCC), needed for proper AVC conduction [21, 50]. The electrocardiogram of *island beat* embryos closely mimic the observed excitation generation in *Setd5* morphants, illustrating a potential AVC disorder due to *Setd5* loss [21, 50]. Secondly, insufficient electrical excitation can be caused by structural alterations within the ventricular myocardium. Excitation propagation is dependent on ventricular trabeculation, since zebrafish hearts lack the complex human ventricular conduction system of His bundle and purkinje fibers [46]. Therefore,

perturbed ventricular trabeculation, as found in the mouse model [39], is known to influence electrical conduction in the ventricular myocardium, which was impaired in the zebrafish *setd5* morphants [46]. Although no alteration in ventricular myocardium was found at 48hpf (see 3.6), further studies should investigate the process of ventricular trabeculation in *setd5* morphants at later stages of development.

4.3 *Setd5* influences the chromatin state

Epigenetic transcriptional regulation is dependent on a continuous balance between histone methylation and acetylation [48]. Of all five histone families, histone 3 and 4 are predominantly targets of posttranslational modifications such as methylation or acetylation [63]. The SET domain containing family is known to methylate lysines of histone tails, but for subfamily VIII comprising *SETD5*, histone methyltransferase (HMT) activity has neither been proven nor denied. Some authors predict an HMT activity of *SETD5* simply based on sequence homology to other SET domain-containing proteins [13, 34, 41].

Western Blot analysis of protein lysates obtained from whole zebrafish embryos at 72hpf did not reveal a difference in methylation status of overall lysine methylation between control or *Setd5* knockdown. Focusing on only histone H3 methylation status, Western Blotting revealed an increase in methylation after *setd5* knockdown (see 3.10, A). These results concur well with Western Blot analysis of protein lysates of embryonic stem cells from *Setd5* knockout mice. Osipovich *et al.* described elevated methylation levels of different tested lysine residues of histone H3 in cells lacking *Setd5* [39]. Therefore, it can be concluded that *Setd5* may lack HMT activity, but nevertheless *Setd5* is involved in the regulation of histone methylation. Underlining this hypothesis, *SETD5* orthologues in yeast, drosophila and mammals were also not found to possess HMT activity [39]. Furthermore, the *SETD5* orthologue *UpSET* in *drosophila* evidently lacks key amino acids required for the catalytic function as HMT [48], supporting the idea that *SETD5* might not function as HMT. Focusing on the entire SET domain family, some other proteins were also found to be devoid of any HMT activity [55]. To date no histone methyltransferase activity of *SETD5* has been experimentally proven [23].

Discussion

Focusing on histone acetylation levels, experiments in *setd5* orthologues showed an increase in histone acetylation in cells lacking *setd5*. For example, a lack of *UpSET*, the *setd5* orthologue in drosophila, led to an elevated acetylation level of histone 3 in Western Blot analysis [48]. Furthermore, Osipovich *et al.* showed an increased pan histone 3 acetylation in embryonic stem cells of *Setd5* knockout mice by Western blotting [39]. Hence, it was interesting to check on histone acetylation in *setd5* knockdown zebrafish embryos. Surprisingly, Western Blotting of whole fish protein lysates revealed a decrease of histone 4 acetylation (see 3.10, B). Interpretation of the obtained findings is difficult, since acetylation levels were analyzed on different histones and in different tissues. Whereas the zebrafish protein lysates contained all proteins from a differentiated fish at 72hpf, Osipovich *et al.* used undifferentiated embryonic stem cells from mice. Future work on *setd5* definitely needs to fully illuminate the influence of *setd5* on histone acetylation. Histone 3 and 4 acetylation levels need to be evaluated throughout the different stages of development since *setd5* seems to be clearly involved in histone acetylation. The orthologues *Set3p* in yeast, *UpSET* in drosophila and *Setd5* in mice, are all found to restrict the recruitment of histone deacetyltransferase (HDAC) complexes to transcriptional start sites to limit active chromatin marks to promotor sites [39, 48]. Consequently, loss of *Setd5* increases histone acetylation at the transcriptional start site and extends active chromatin marks in the direction of the 3' end of the gene [39, 48].

In summary, the results suggest that *Setd5* is required for chromatin accessibility and might be involved in the process of histone methylation and acetylation. Therefore, a loss of *Setd5* leads to an epigenetic imbalance [39].

4.4 *Setd5* presumably functions in Notch Signaling

Several major interaction partners of *setd5* have been described, placing *Setd5* protein function in context to the highly evolutionary conserved cell-to-cell Notch signaling pathway. As stated above, *SETD5* orthologues have been shown to be involved in HDAC recruitment to transcriptional start sites [39, 48]. HDACs actively repress gene transcription by functioning as large multiprotein complexes who interact with DNA binding proteins [14].

Discussion

Mass spectrometry analysis from Osipovich *et al.* revealed that FLAG-setd5 co-precipitates with members of such DNA binding complexes. Direct interaction of Setd5 has been described for members of the PAF1C complex and members of the NCoR co-repressor complex [39]. The NCoR co-repressor complex in mammals is made up of NCOR1/NCOR2 (SMRT), HDAC3 and WD40 repeat containing proteins (TBL1X and TBL1XR1) among others [39]. This Co-Repressor complex silences gene expression and has shown to be essential in development of multiple organ systems, including the heart and nervous system [39]. In yeast, the *setd5* orthologue *Set3p* has been identified as a component of the yeast orthologue of the NCoR-co-repressor complex [39]. In mammals, no SET domain containing protein has been found to interact with the NCoR co-repressor complex [39]. Being the vertebrate orthologue of *Set3p*, *SETD5* might be the looked-for interaction partner of the NCoR co-repressor complex, since loss of *SETD5* leads to neural and cardiac defects in zebrafish and mice (see 3.2) [39].

Additionally, Setd5 has been shown to interact with the SPEN Paralog and Ortholog C-terminal domain of SPEN (SPOC) (or otherwise referred to as SHARP or MINT) in a yeast-two-hybrid screening (personal communication Prof. Dr. rer. nat. Franz Oswald, Department of Internal Medicine I, University Medical Center Ulm).

The three stated findings of Setd5 interaction with HDACs [39, 48], the NCoR co-repressor complex [39] and the RNA recognition motif of SHARP (personal communication Prof. Dr. rer. nat. Franz Oswald) suggest a function of *SETD5* in the Notch signaling pathway.

The Notch signaling pathway is one of a few evolutionary highly conserved signal transduction pathways [5, 22, 30, 37]. Through ligand receptor interaction, the intracellular receptor domain NICD (Notch intracellular domain) gets cleaved and binds the nuclear effector of the pathway, the DNA binding protein CSL (RBP-J, CBF-1, Su(H), Lag-1) [60]. CSL functions as a molecular switch, either repressing or activating the transcription of Notch target genes by binding to co-repressor complexes or co-activation proteins and coordinating chromatin modifications [5, 10, 60]. In absence of nuclear NICD, the transcriptional co-repressor SHARP (=SMRT/ HDAC repressor protein) directly interacts with CSL. SHARP's SPOC domain recruits NCoR (SMRT) co-repressor complexes, which both interact with

Discussion

Setd5 [4, 32, 60]. NCoR serves as a platform for recruiting other large transcription repression complexes including histone deacetylases, creating a repressive chromatin environment [4, 32].

During embryogenesis, the heart is the first organ to form and function [37]. Cell fate specification and tissue patterning are under control of the Notch signaling pathway, which functions in the heart during cardiac development, congenital heart disease and heart regeneration [30]. Cardiac notch signaling in the developing heart regulates out flow tract (OFT) development, AVC boundary and valve formation, as well as endocardial and ventricular myocardial maturation [37]. As mentioned above, the observed silent ventricle phenotype can be caused by AVC malformation or impaired ventricular trabeculation in which Notch signaling is involved (see 4.2).

Proper AVC conduction is dependent on endocardial signals of notch1b and neuregulin [46, 67]. Notch1b is required for the central conduction system in the forming heart, being responsible for the slow impulse generation and prolonged refractory periods, needed for the characteristic AVC delay [33]. Both loss and gain of function mutations in the notch signaling pathway have been shown to result in defects during AVC development [37].

Furthermore, loss of *SETD5* in mice and zebrafish caused restrained ventricular trabeculation, leading to a lack of chamber contraction [39]. The endocardial Notch signaling regulates ventricular myocardial development including trabeculation and therefore might be affected in Setd5 morphants, again underlining a possible function of Setd5 within Notch signaling [37]. The hypothesized function of Setd5 during the recruitment of HDACs is also in accordance with the observed ventricular malfunction of *Setd5* morphant embryos. HDACs are known to modulate contractile function through posttranslational deacetylation of contractile and structural proteins [66].

In summary, the literature provides strong evidence that Setd5 interacts with certain members of the Notch co-repressor complex. To date, further analysis of a possible Setd5 function within the Notch signaling pathway is lacking. Only Rincon-Arano *et al.* stated, that the *Setd5* orthologue *UpSET* modulates Notch signaling in *Drosophila* [48].

5 Summary

Cardiovascular diseases are the leading cause of death worldwide. Changes in chromatin structure alter gene expression and drive cardiovascular disease pathogenesis. The SET ((Su(var)3-9), enhancer of zeste (E(z)) and trithorax (Trx)) domain-containing protein family is such a group of chromatin modifiers, who are known to methylate histones. The SET domain-containing protein 5 (*setd5*) is a member of this family and was previously connected to cardiovascular disease generation in mouse.

The purpose of the presented thesis was to further characterize the role of Setd5 in vertebrate heart development. Since embryonic mice are not viable without a functional cardiovascular system, the zebrafish was chosen as a model organism because of its ease of genetic manipulation and the ability to survive without a functional cardiovascular system.

Setd5 deficiency, generated by Morpholino-modified antisense oligonucleotide injection in zebrafish embryos, resulted in severe cardiac defects. Although no impairment in heart differentiation and specification was evident, the observed heart morphology was highly altered. Atria appeared stretched and thin, whereas the ventricle presented a compact and lumpy conformation. Functional analysis showed that Setd5 is essential to maintain cardiac contractile function in zebrafish. Loss of Setd5 led to a distinct phenotype, mainly a silent ventricle and atrial arrhythmia. Analysis of the cardiac conduction system showed regular excitation propagation in the atrium and dysfunctional electrical excitation of ventricular cardiomyocytes. Focusing on chromatin modification, knockdown of *setd5* led to increased methylation and reduced acetylation of histones.

In conclusion, loss of *setd5* impairs cardiac morphology and function *in vivo*.

6 References

1. Arnaout R, Ferrer T, Huisken J, Spitzer K, Stainier DY, Tristani-Firouzi M, Chi NC: Zebrafish model for human long QT syndrome. *Proc Natl Acad Sci U S A* 104: 11316-11321 (2007)
2. Barut BA, Zon LI: Realizing the potential of zebrafish as a model for human disease. *Physiol Genomics* 2: 49-51 (2000)
3. Bauer AJ, Martin KA: Coordinating Regulation of Gene Expression in Cardiovascular Disease: Interactions between Chromatin Modifiers and Transcription Factors. *Front Cardiovasc Med* 4: 19 (2017)
4. Borggreffe T, Oswald F: Keeping notch target genes off: a CSL corepressor caught in the act. *Structure* 22: 3-5 (2014)
5. Borggreffe T, Oswald F: Setting the Stage for Notch: The Drosophila Su(H)-Hairless Repressor Complex. *PLoS Biol* 14: e1002524 (2016)
6. Cosgrove MS, Wolberger C: How does the histone code work? *Biochem Cell Biol* 83: 468-476 (2005)
7. Dahme T, Katus HA, Rottbauer W: Fishing for the genetic basis of cardiovascular disease. *Dis Model Mech* 2: 18-22 (2009)
8. Dillon SC, Zhang X, Trievel RC, Cheng X: The SET-domain protein superfamily: protein lysine methyltransferases. *Genome Biol* 6: 227 (2005)
9. Eisen JS, Smith JC: Controlling morpholino experiments: don't stop making antisense. *Development* 135: 1735-1743 (2008)
10. Giaimo BD, Oswald F, Borggreffe T: Dynamic chromatin regulation at Notch target genes. *Transcription* 8: 61-66 (2017)
11. Gillette TG, Hill JA: Readers, writers, and erasers: chromatin as the whiteboard of heart disease. *Circ Res* 116: 1245-1253 (2015)
12. Gottlieb PD, Pierce SA, Sims RJ, Yamagishi H, Weihe EK, Harriss JV, Maika SD, Kuziel WA, King HL, Olson EN, Nakagawa O, Srivastava D: Bop encodes a muscle-restricted protein containing MYND and SET domains and

References

- is essential for cardiac differentiation and morphogenesis. *Nat Genet* 31: 25-32 (2002)
13. Grozeva D, Carss K, Spasic-Boskovic O, Parker MJ, Archer H, Firth HV, Park SM, Canham N, Holder SE, Wilson M, Hackett A, Field M, Floyd JA, Consortium UK, Hurles M, Raymond FL: De novo loss-of-function mutations in SETD5, encoding a methyltransferase in a 3p25 microdeletion syndrome critical region, cause intellectual disability. *Am J Hum Genet* 94: 618-624 (2014)
 14. Guenther MG, Barak O, Lazar MA: The SMRT and N-CoR corepressors are activating cofactors for histone deacetylase 3. *Mol Cell Biol* 21: 6091-6101 (2001)
 15. Hassel D, Scholz EP, Trano N, Friedrich O, Just S, Meder B, Weiss DL, Zitron E, Marquart S, Vogel B, Karle CA, Seemann G, Fishman MC, Katus HA, Rottbauer W: Deficient zebrafish ether-a-go-go-related gene channel gating causes short-QT syndrome in zebrafish reggae mutants. *Circulation* 117: 866-875 (2008)
 16. Howe K, Clark MD, Torroja CF, Torrance J, Berthelot C, Muffato M, Collins JE, Humphray S, McLaren K, Matthews L, McLaren S, Sealy I, Caccamo M, Churcher C, Scott C, Barrett JC, Koch R, Rauch GJ, White S, Chow W, Kilian B, Quintais LT, Guerra-Assuncao JA, Zhou Y, Gu Y, Yen J, Vogel JH, Eyre T, Redmond S, Banerjee R, Chi J, Fu B, Langlely E, Maguire SF, Laird GK, Lloyd D, Kenyon E, Donaldson S, Sehra H, Almeida-King J, Loveland J, Trevanion S, Jones M, Quail M, Willey D, Hunt A, Burton J, Sims S, McLay K, Plumb B, Davis J, Clee C, Oliver K, Clark R, Riddle C, Elliot D, Threadgold G, Harden G, Ware D, Begum S, Mortimore B, Kerry G, Heath P, Phillimore B, Tracey A, Corby N, Dunn M, Johnson C, Wood J, Clark S, Pelan S, Griffiths G, Smith M, Glithero R, Howden P, Barker N, Lloyd C, Stevens C, Harley J, Holt K, Panagiotidis G, Lovell J, Beasley H, Henderson C, Gordon D, Auger K, Wright D, Collins J, Raisen C, Dyer L, Leung K, Robertson L, Ambridge K, Leongamornlert D, McGuire S, Gilderthorp R, Griffiths C, Manthravadi D, Nichol S, Barker G, Whitehead S, Kay M, Brown J, Murnane C, Gray E, Humphries M, Sycamore N, Barker D, Saunders D, Wallis J,

References

- Babbage A, Hammond S, Mashreghi-Mohammadi M, Barr L, Martin S, Wray P, Ellington A, Matthews N, Ellwood M, Woodmansey R, Clark G, Cooper J, Tromans A, Grafham D, Skuce C, Pandian R, Andrews R, Harrison E, Kimberley A, Garnett J, Fosker N, Hall R, Garner P, Kelly D, Bird C, Palmer S, Gehring I, Berger A, Dooley CM, Ersan-Urun Z, Eser C, Geiger H, Geisler M, Karotki L, Kirn A, Konantz J, Konantz M, Oberlander M, Rudolph-Geiger S, Teucke M, Lanz C, Raddatz G, Osoegawa K, Zhu B, Rapp A, Widaa S, Langford C, Yang F, Schuster SC, Carter NP, Harrow J, Ning Z, Herrero J, Searle SM, Enright A, Geisler R, Plasterk RH, Lee C, Westerfield M, de Jong PJ, Zon LI, Postlethwait JH, Nusslein-Volhard C, Hubbard TJ, Roest Crollius H, Rogers J, Stemple DL: The zebrafish reference genome sequence and its relationship to the human genome. *Nature* 496: 498-503 (2013)
17. Iwasaki YK, Nishida K, Kato T, Nattel S: Atrial fibrillation pathophysiology: implications for management. *Circulation* 124: 2264-2274 (2011)
 18. Jan Behrends JB, Rainer Deutzmann, Heimo Ehmke, Stephan Frings, Stephan Grissmer, Markus Hoth, Armin Kurtz, Jens Leipziger, Frank Müller, Claudia Pedain, Jens Rettig, Charlotte Wagner, Erhard Wischmeyer: *Duale-Reihe: Physiologie. Bd 1*, Thieme, Stuttgart, p.73-106 (2010)
 19. Jenuwein T, Laible G, Dorn R, Reuter G: SET domain proteins modulate chromatin domains in eu- and heterochromatin. *Cell Mol Life Sci* 54: 80-93 (1998)
 20. Kellogg G, Sum J, Wallerstein R: Deletion of 3p25.3 in a patient with intellectual disability and dysmorphic features with further definition of a critical region. *Am J Med Genet A* 161A: 1405-1408 (2013)
 21. Kessler M, Just S, Rottbauer W: Ion flux dependent and independent functions of ion channels in the vertebrate heart: lessons learned from zebrafish. *Stem Cells Int* 2012: 462161 (2012)
 22. Kopan R, Ilagan MX: The canonical Notch signaling pathway: unfolding the activation mechanism. *Cell* 137: 216-233 (2009)
 23. Kuechler A, Zink AM, Wieland T, Ludecke HJ, Cremer K, Salviati L, Magini P, Najafi K, Zweier C, Czeschik JC, Aretz S, Ende S, Tamburrino F, Pinato C, Clementi M, Gundlach J, Maylahn C, Mazzanti L, Wohlleber E, Schwarzmayr

References

- T, Kariminejad R, Schlessinger A, Wieczorek D, Strom TM, Novarino G, Engels H: Loss-of-function variants of SETD5 cause intellectual disability and the core phenotype of microdeletion 3p25.3 syndrome. *Eur J Hum Genet* 23: 753-760 (2015)
24. Kwan KM, Fujimoto E, Grabher C, Mangum BD, Hardy ME, Campbell DS, Parant JM, Yost HJ, Kanki JP, Chien CB: The Tol2kit: a multisite gateway-based construction kit for Tol2 transposon transgenesis constructs. *Dev Dyn* 236: 3088-3099 (2007)
25. Lawson ND, Weinstein BM: In vivo imaging of embryonic vascular development using transgenic zebrafish. *Dev Biol* 248: 307-318 (2002)
26. Li H, Zhong Y, Wang Z, Gao J, Xu J, Chu W, Zhang J, Fang S, Du SJ: Smyd1b is required for skeletal and cardiac muscle function in zebrafish. *Mol Biol Cell* 24: 3511-3521 (2013)
27. Li M, Zhao L, Page-McCaw PS, Chen W: Zebrafish Genome Engineering Using the CRISPR-Cas9 System. *Trends Genet* 32: 815-827 (2016)
28. Lieschke GJ, Currie PD: Animal models of human disease: zebrafish swim into view. *Nat Rev Genet* 8: 353-367 (2007)
29. Liu J, Zhou Y, Qi X, Chen J, Chen W, Qiu G, Wu Z, Wu N: CRISPR/Cas9 in zebrafish: an efficient combination for human genetic diseases modeling. *Hum Genet* 136: 1-12 (2017)
30. Luxan G, D'Amato G, MacGrogan D, de la Pompa JL: Endocardial Notch Signaling in Cardiac Development and Disease. *Circ Res* 118: e1-e18 (2016)
31. Mendis SP, P.; Norrving, B . Global Atlas on Cardiovascular Disease Prevention and Control. (2011)
32. Mikami S, Kanaba T, Ito Y, Mishima M: NMR assignments of SPOC domain of the human transcriptional corepressor SHARP in complex with a C-terminal SMRT peptide. *Biomol NMR Assign* 7: 267-270 (2013)
33. Milan DJ, Giokas AC, Serluca FC, Peterson RT, MacRae CA: Notch1b and neuregulin are required for specification of central cardiac conduction tissue. *Development* 133: 1125-1132 (2006)

References

34. Morimoto A, Kannari M, Tsuchida Y, Sasaki S, Saito C, Matsuta T, Maeda T, Akiyama M, Nakamura T, Sakaguchi M, Nameki N, Gonzalez FJ, Inoue Y: An HNF4 α -microRNA-194/192 Signaling Axis Maintains Hepatic Cell Function. *J Biol Chem* (2017)
35. Mozaffarian D, Benjamin EJ, Go AS, Arnett DK, Blaha MJ, Cushman M, Das SR, de Ferranti S, Despres JP, Fullerton HJ, Howard VJ, Huffman MD, Isasi CR, Jimenez MC, Judd SE, Kissela BM, Lichtman JH, Lisabeth LD, Liu S, Mackey RH, Magid DJ, McGuire DK, Mohler ER, 3rd, Moy CS, Muntner P, Mussolino ME, Nasir K, Neumar RW, Nichol G, Palaniappan L, Pandey DK, Reeves MJ, Rodriguez CJ, Rosamond W, Sorlie PD, Stein J, Towfighi A, Turan TN, Virani SS, Woo D, Yeh RW, Turner MB: Heart Disease and Stroke Statistics-2016 Update: A Report From the American Heart Association. *Circulation* 133: e38-360 (2016)
36. Nasevicius A, Ekker SC: Effective targeted gene 'knockdown' in zebrafish. *Nat Genet* 26: 216-220 (2000)
37. Niessen K, Karsan A: Notch signaling in cardiac development. *Circ Res* 102: 1169-1181 (2008)
38. Nishikawa K, Kinjo AR: Essential role of long non-coding RNAs in de novo chromatin modifications: the genomic address code hypothesis. *Biophys Rev* 9: 73-77 (2017)
39. Osipovich AB, Gangula R, Vianna PG, Magnuson MA: Setd5 is essential for mammalian development and the co-transcriptional regulation of histone acetylation. *Development* 143: 4595-4607 (2016)
40. Paone C, Rudeck S, Etard C, Strahle U, Rottbauer W, Just S: Loss of zebrafish *Smyd1a* interferes with myofibrillar integrity without triggering the misfolded myosin response. *Biochem Biophys Res Commun* 496: 339-345 (2018)
41. Parenti I, Teresa-Rodrigo ME, Pozojevic J, Ruiz Gil S, Bader I, Braunholz D, Bramswig NC, Gervasini C, Larizza L, Pfeiffer L, Ozkinay F, Ramos F, Reiz B, Rittinger O, Strom TM, Watrin E, Wendt K, Wieczorek D, Wollnik B, Baquero-Montoya C, Pie J, Deardorff MA, Gillessen-Kaesbach G, Kaiser FJ: Mutations in chromatin regulators functionally link Cornelia de Lange

References

- syndrome and clinically overlapping phenotypes. *Hum Genet* 136: 307-320 (2017)
42. Peltekova IT, Macdonald A, Armour CM: Microdeletion on 3p25 in a patient with features of 3p deletion syndrome. *Am J Med Genet A* 158a: 2583-2586 (2012)
43. Pfeiffer ER, Tangney JR, Omens JH, McCulloch AD: Biomechanics of cardiac electromechanical coupling and mechanoelectric feedback. *J Biomech Eng* 136: 021007 (2014)
44. Pinto D, Delaby E, Merico D, Barbosa M, Merikangas A, Klei L, Thiruvahindrapuram B, Xu X, Ziman R, Wang Z, Vorstman JA, Thompson A, Regan R, Pilorge M, Pellecchia G, Pagnamenta AT, Oliveira B, Marshall CR, Magalhaes TR, Lowe JK, Howe JL, Griswold AJ, Gilbert J, Duketis E, Dombroski BA, De Jonge MV, Cuccaro M, Crawford EL, Correia CT, Conroy J, Conceicao IC, Chiocchetti AG, Casey JP, Cai G, Cabrol C, Bolshakova N, Bacchelli E, Anney R, Gallinger S, Cotterchio M, Casey G, Zwaigenbaum L, Wittemeyer K, Wing K, Wallace S, van Engeland H, Tryfon A, Thomson S, Soorya L, Roge B, Roberts W, Poustka F, Mougá S, Minshew N, McInnes LA, McGrew SG, Lord C, Leboyer M, Le Couteur AS, Kolevzon A, Jimenez Gonzalez P, Jacob S, Holt R, Guter S, Green J, Green A, Gillberg C, Fernandez BA, Duque F, Delorme R, Dawson G, Chaste P, Cafe C, Brennan S, Bourgeron T, Bolton PF, Bolte S, Bernier R, Baird G, Bailey AJ, Anagnostou E, Almeida J, Wijsman EM, Veland VJ, Vicente AM, Schellenberg GD, Pericak-Vance M, Paterson AD, Parr JR, Oliveira G, Nurnberger JI, Monaco AP, Maestrini E, Klauck SM, Hakonarson H, Haines JL, Geschwind DH, Freitag CM, Folstein SE, Ennis S, Coon H, Battaglia A, Szatmari P, Sutcliffe JS, Hallmayer J, Gill M, Cook EH, Buxbaum JD, Devlin B, Gallagher L, Betancur C, Scherer SW: Convergence of genes and cellular pathways dysregulated in autism spectrum disorders. *Am J Hum Genet* 94: 677-694 (2014)
45. Poon KL, Liebling M, Kondrychyn I, Garcia-Lecea M, Korzh V: Zebrafish cardiac enhancer trap lines: new tools for in vivo studies of cardiovascular development and disease. *Dev Dyn* 239: 914-926 (2010)

References

46. Poon KL, Brand T: The zebrafish model system in cardiovascular research: A tiny fish with mighty prospects. *Glob Cardiol Sci Pract* 2013: 9-28 (2013)
47. Rice JC, Allis CD: Code of silence. *Nature* 414: 258-261 (2001)
48. Rincon-Arano H, Halow J, Delrow JJ, Parkhurst SM, Groudine M: UpSET recruits HDAC complexes and restricts chromatin accessibility and acetylation at promoter regions. *Cell* 151: 1214-1228 (2012)
49. Rosa-Garrido M, Karbassi E, Monte E, Vondriska TM: Regulation of chromatin structure in the cardiovascular system. *Circ J* 77: 1389-1398 (2013)
50. Rottbauer W, Baker K, Wo ZG, Mohideen MA, Cantiello HF, Fishman MC: Growth and function of the embryonic heart depend upon the cardiac-specific L-type calcium channel alpha1 subunit. *Dev Cell* 1: 265-275 (2001)
51. Sander V, Sune G, Jopling C, Morera C, Izpisua Belmonte JC: Isolation and in vitro culture of primary cardiomyocytes from adult zebrafish hearts. *Nat Protoc* 8: 800-809 (2013)
52. Santoriello C, Zon LI: Hooked! Modeling human disease in zebrafish. *J Clin Invest* 122: 2337-2343 (2012)
53. Stainier DY, Fishman MC: The zebrafish as a model system to study cardiovascular development. *Trends Cardiovasc Med* 4: 207-212 (1994)
54. Stainier DY, Fouquet B, Chen JN, Warren KS, Weinstein BM, Meiler SE, Mohideen MA, Neuhauss SC, Solnica-Krezel L, Schier AF, Zwartkruis F, Stemple DL, Malicki J, Driever W, Fishman MC: Mutations affecting the formation and function of the cardiovascular system in the zebrafish embryo. *Development* 123: 285-292 (1996)
55. Sun XJ, Xu PF, Zhou T, Hu M, Fu CT, Zhang Y, Jin Y, Chen Y, Chen SJ, Huang QH, Liu TX, Chen Z: Genome-wide survey and developmental expression mapping of zebrafish SET domain-containing genes. *PLoS One* 3: e1499 (2008)
56. Szczaluba K, Brzezinska M, Kot J, Rydzanicz M, Walczak A, Stawinski P, Werner B, Ploski R: SETD5 loss-of-function mutation as a likely cause of a

References

- familial syndromic intellectual disability with variable phenotypic expression. *Am J Med Genet A* 170: 2322-2327 (2016)
57. Tessadori F, van Weerd JH, Burkhard SB, Verkerk AO, de Pater E, Boukens BJ, Vink A, Christoffels VM, Bakkers J: Identification and functional characterization of cardiac pacemaker cells in zebrafish. *PLoS One* 7: e47644 (2012)
 58. Thisse C, Thisse B: High-resolution in situ hybridization to whole-mount zebrafish embryos. *Nat Protoc* 3: 59-69 (2008)
 59. Timme-Laragy AR, Karchner SI, Hahn ME: Gene knockdown by morpholino-modified oligonucleotides in the zebrafish (*Danio rerio*) model: applications for developmental toxicology. *Methods Mol Biol* 889: 51-71 (2012)
 60. VanderWielen BD, Yuan Z, Friedmann DR, Kovall RA: Transcriptional repression in the Notch pathway: thermodynamic characterization of CSL-MINT (Msx2-interacting nuclear target protein) complexes. *J Biol Chem* 286: 14892-14902 (2011)
 61. Westerfield M: THE ZEBRAFISH BOOK
A guide for the laboratory use of zebrafish (*Danio rerio*). Bd 4th edition, University of Oregon Press, Eugene, p.4-6 (2000)
 62. Xiao B, Wilson JR, Gamblin SJ: SET domains and histone methylation. *Curr Opin Struct Biol* 13: 699-705 (2003)
 63. Yan C, Boyd DD: Histone H3 acetylation and H3 K4 methylation define distinct chromatin regions permissive for transgene expression. *Mol Cell Biol* 26: 6357-6371 (2006)
 64. Yang J, Xu X: Immunostaining of dissected zebrafish embryonic heart. *J Vis Exp* e3510 (2012)
 65. Zhang D, Wu CT, Qi X, Meijering RA, Hoogstra-Berends F, Tadevosyan A, Cubukcuoglu Deniz G, Durdu S, Akar AR, Sibon OC, Nattel S, Henning RH, Brundel BJ: Activation of histone deacetylase-6 induces contractile dysfunction through derailment of alpha-tubulin proteostasis in experimental and human atrial fibrillation. *Circulation* 129: 346-358 (2014)

References

66. Zhang D, Hu X, Henning RH, Brundel BJ: Keeping up the balance: role of HDACs in cardiac proteostasis and therapeutic implications for atrial fibrillation. *Cardiovasc Res* 109: 519-526 (2016)
67. Zhou XL, Liu JC: Role of Notch signaling in the mammalian heart. *Braz J Med Biol Res* 47: 1-10 (2014)

Acknowledgements

This page was removed for privacy reasons.

Statutory declaration

I hereby declare that I wrote the present dissertation with the topic:

**“Targeted loss of SET domain-containing protein 5
impairs cardiac morphology and function *in vivo*”**

independently and used no other aids than those cited. In each individual case, I have clearly identified the source of the passages that are taken word for word or paraphrased from other works.

I also hereby declare that I have carried out my scientific work according to the principles of good scientific practice in accordance with the current “Satzung der Universität Ulm zur Sicherung guter wissenschaftlicher Praxis“ (Rules of the University of Ulm for Assuring Good Scientific Practice).

Ulm,

(Sabine Schreiber)

Curriculum vitae

This page was removed for privacy reasons.